Journal of Volcanology and Geothermal Research 371 (2019) 72–85

Contents lists available at ScienceDirect

Journal of Volcanology and Geothermal Research

journal homepage: www.elsevier.com/locate/jvolgeores

# The $\delta^{18}O$ of primary and secondary waters in hydrous volcanic glass

Angela N. Seligman, Ilya N. Bindeman *

*Department of Geological Sciences, 1272 University of Oregon, Eugene, OR 97403-1272, USA*

ARTICLE INFO

*Article history:*
Received 9 August 2018
Received in revised form 21 December 2018
Accepted 21 December 2018
Available online 3 January 2019

*Keywords:*
Oxygen isotopes
Hydrogen isotopes
Volcanic glass
TCEA
Volcanic degassing
Secondary hydration

ABSTRACT

We present analyses of phyllosilicates, volcanic glass, and a series of experiments and observations on the $\delta^{18}O$ of water extracted by rapid thermal pyrolysis at 1450 °C using the TCEA (Thermal Conversion Elemental Analyzer). The study includes the same hydrous glasses that were previously analyzed for their δD values of extracted water (Seligman et al., 2016). We utilize natural phyllosilicates (where water is present as $OH^-$ only), natural magmatic and experimentally quenched glasses, (in which water occurs as $H_2O_m$ and $OH^-$), and glasses that underwent low-temperature secondary hydration by meteoric water (almost completely as $H_2O_m$). Our study documents that: 1) thermal extraction and simultaneous pyrolysis of $H_2O_t$ into CO and $H_2$ produces little or no exchange (<1‰) in $\delta^{18}O$ between hydrogen-bound and silica-bound oxygen; 2) water extracted from different natural phyllosilicates have $10^3\ln\alpha_{silicate\text{-}OH}$ ($\sim\delta^{18}O_{silicate} - \delta^{18}O_{OH}$) values ranging from −3 to 6‰, which is in agreement with previous results using partial fluorination, Density-Functional Theory, and the increment method; 3) water extracted from eruptively or experimentally quenched hydrous magmatic glasses have $10^3\ln\alpha_{silicate\text{-}H2Ot}$ values that decrease with increasing quench temperature from 10‰ (900 °C) to 3‰ (1100 °C); 4) during progressive volcanic degassing, the $\delta^{18}O$ of remaining water in glass decrease as the departing $H_2O_m$ is more positive in $\delta^{18}O$, especially at lower temperature; this oxygen isotope trend correlates with δD as the departing $H_2O_m$ is also more positive in δD than the remaining magmatic water. 5) the $\delta^{18}O$ of water extracted from glass hydrated at low-temperature by secondary water yields isotopically negative $\delta^{18}O$ values that are closer to the $\delta^{18}O$ values of local meteoric water than values appropriate for low temperature silicate-water $^{18}O/^{16}O$ equilibrium; this suggests that upon hydration water simply dissolves into glass as $H_2O$; 6) subsequently, secondarily hydrated glasses appear to show an increase in $\delta^{18}O$ values that trend towards equilibrium with continued secondary hydration, with time, and at higher temperatures. This research demonstrates that the $\delta^{18}O$ of extracted water, despite its 1–2 per mil- analytical precision, provides an isotopic tool for investigations of first order trends of both magmatic degassing, and of secondary hydration by meteoric waters. The trends described here aids hydrogen isotopic variations in the same processeses and combined use of both O and H isotopic variation of water in glass to help fingerprint sources of meteoric water, extent and stages of alteration of glass, and magmatic degassing.



## 1. Introduction

### 1.1. Oxygen isotopes of water extracted from hydrous silicates

Investigations of oxygen isotopes of water from hydrous silicates, oxides, and sulfates (e.g. kaolinite, goethite, illite, other micas, and alunite), was attempted in the early days of stable isotope geochemistry in addition to the bulk $\delta^{18}O$ analysis of these phases (Savin, 1967; Hamza and Epstein, 1980; Yapp, 1987; Bechtel and Hoernes, 1990; Girard and Savin, 1996; Gilg et al., 2004). The main motivating factor of these studies is to use these minerals as recorders of $\delta^{18}O$ and δD values of equilibrium water, and thus paleoclimate, provided that the temperature of interaction and isotopic fractionations are established. Just as bulk $\delta^{18}O$ values of a hydrous phase in conjunction with δD can in theory resolve both the isotopic values of water and temperature (Yapp, 1987), the intra-structure fractionation of $\delta^{18}O$ between hydrogen- and silicate-bound oxygen can potentially also serve this purpose (Hamza and Epstein, 1980; Bechtel and Hoernes, 1990). The hydrogen-bound oxygen will have a unique fractionation from the oxygen in the silicate, which depends on the phase, the temperature at which it was acquired, or isotopically closed to exchange. Internal silicate-OH $\delta^{18}O$ fractionation were thought to serve as a single-mineral isotope thermometer (recording the temperature of last equilibration or isotopic closure), comparatively similar to modern day clumped isotope methods (Eiler, 2007).

In order to extract hydrogen-bound oxygen from clays and other OH- and $H_2O$-bearing materials, two chief methods were previously employed: 1) partial low-temperature fluorination using $F_2$ gas (Hamza and Epstein, 1980; Yapp, 1987; Bechtel and Hoernes, 1990)

* Corresponding author at: Department of Earth Sciences, 1272 University of Oregon, Eugene, OR 97403-1272, USA.
*E-mail addresses:* seligman@uoregon.edu (A.N. Seligman), bindeman@uoregon.edu (I.N. Bindeman).

https://doi.org/10.1016/j.jvolgeores.2018.12.008
0377-0273/

and 2) thermal dehydroxylation by heating in a resistance furnace conducted at 500–1000 °C (Girard and Savin, 1996; Sheppard and Gilg, 1996 and references therein). Both methods, coupled with measurements of $\delta^{18}O$ in the silicate residue, yielded good mass balance constraints and results carried 1–2‰ $\delta^{18}O$ analytical uncertainties. Both Hamza and Epstein (1980) and Bechtel and Hoernes (1990) used off-line, "conventional" extraction and analytical techniques and rather large quantities of material, and found that fluorination and thermal dehydroxylation yielded overlapping results, while Girard and Savin (1996) and Clayton and Mayeda (2009) suggested that thermal dehydroxylation is preferred. Despite the rather large amount of material used (10s to 100s of mg), these authors suggested that there is insignificant isotopic exchange between the residual silicate and the departing water upon rapid water extraction from the sample. Therefore, the resulting $10^3\ln\alpha_{silicate\text{-}OH}$ reflects the true fractionation between the OH-bound oxygen and the silicate oxygen, thus retrieving $\delta^{18}O_{water}$ values, $10^3\ln\alpha_{silicate\text{-}OH}$ fractionations, and the final diffusional closure temperature of the two types of oxygen. However, since only half of the oxygen is extracted as $H_2O$ from the $OH^-$ sites during dehydroxylation ($\boldsymbol{2OH^- = H_2O_m + O_{silicate}^{2-}}$), the measured difference requires correction using the fractionation at the temperature of extraction, a topic that we explore in detail below. The added step of correcting for the residual oxygen in the silicate and the concern for isotopic exchange during heating and analysis are possible reasons why these earlier methods are not widely utilized.

Another approach to understand water (and $OH^-$) fractionation in silicates is to use theoretical or semi-empirical approaches (e.g. increment method) involving oxygen bonding environments and the associated dependence on temperature. Using these methods, Schütze (1984) and Zheng (1993a) computed OH-phyllosilicate fractionations as a function of temperature. Girard and Savin (1996) and Bechtel and Hoernes (1990) observed that their experimentally determined OH-silicate fractionations agree with these calculations at 200–300 °C, which is the presumed closure temperature of silicate-OH exchange for these plutonic minerals. However, disagreements were larger for micas formed at low (cooler hydrothermal or ambient) temperatures, which predict, for example, 40‰ oxygen isotopic fractionation between the silicate and the OH-portion of kaolinite (Zheng, 1993a). The closure temperature for the investigated samples, which originated from hydrothermal deposits or plutonic environments, was not discussed by either author.

Méheut et al. (2007, 2010) and Balan et al. (2007) utilized Density-Functional Theory (DFT) simulations to estimate isotopic fractionations between hydrous phyllosillicates and water, and internal isotopic fractionations of oxygen in kaolinite, with a 5% precision. Results from their studies suggest that hydrous minerals (e.g. kaolinite and muscovite) have $10^3\ln\alpha_{silicate\text{-}OH}$ between ~2‰ (kaolinite) and ~1‰ (muscovite) at ~300 °C, and that at lower temperatures the $10^3\ln\alpha_{bulk\text{-}OH}$ become more positive. Collectively, the aforementioned studies provide a background to understand magmatic glass. They however carry both analytical and theoretical controversies that we try to address and resolve in this study.

This paper takes the above-described research further by using a Thermal Conversion Elemental Analyzer (TCEA) continuous flow system that uses glassy carbon coupled with a large radius MAT253 mass spectrometer (Fig. 1, developed after the original design by Sharp et al., 2001). These systems are now available at many Universities and rely on milligram quantities of the freshest concentrate material, representing a reduction in the sample size by 30–100 times compared to conventional methods. The extraction at high 1450 °C temperature and instantaneous reduction of extracted water to CO gas provides advantages over previously used lower temperature (500–1000 °C), multi-step, and off-line methods. The TCEA approach allows less time for syn-extraction exchange between the silicate and water, which is perhaps better than the earlier employed three step process involving initial dehydroxilation followed by water reduction and then off-line isotope analysis. In addition, the TCEA, when coupled to a large radius MAT 253 mass spectrometer, allows for sample sizes of just a few mg with as little as 0.1 wt% water, compared to hundreds of mg required in previously employed conventional methods (Hamza and Epstein, 1980; Bechtel and Hoernes, 1990; Girard and Savin, 1996), or Delta mass spectrometry systems, the latter requiring >0.3 wt% of water and 4× the amount of material for analysis.

### 1.2. Goals of the present study

Despite rather large number of studies of $\delta^{18}O$ in hydrous materials (clays, goethite, sulphates, phosphates) mostly for paleoenvironmental purposes (Vennemann et al., 2002; Bao and Marchant, 2006; Friedman et al., 1993; Cassel et al., 2014; Pingel et al., 2016; Bao et al., 2000), there are currently few studies on the $\delta^{18}O$ value of water extracted from volcanic glass (e.g. Nolan and Bindeman, 2013; Bindeman and Lowenstern, 2016; Hudak and Bindeman, 2018; Seligman et al., 2018), and there are no studies of $\delta^{18}O$ in primary magmatic water left in glass during magmatic degassing. This may be due to the unknown reliability of the analyses, practical utility, and the meaning of the $\delta^{18}O$ of the extracted waters. For decades researchers have worked towards understanding the processes that occur during the diffusion of water into volcanic glass, and to be able to distinguish between primary magmatic and secondary environmental water in volcanic glasses (e.g. Friedman and Long, 1976; Newman et al., 1988; Zhang, 1999; Doremus, 2000; Crovisier et al., 2003; Anovitz et al., 2009; Seligman et al., 2016; Hudak and Bindeman, 2018).

We here test if $\delta^{18}O$ analyses of water in hydrous glasses will be a practical approach to understanding magmatic processes of volcanic degassing, and environmental processes of secondary hydration, which can be correlated with already well-understood hydrogen isotopic systematics (Taylor and Westrich, 1985; Dobson et al., 1989; Friedman and Long, 1976; Seligman et al., 2016). Understanding water concentrations, speciation ($H_2O_m$ and $OH^-$), and the $\delta D$ values of water in rapidly quenched glasses is important in understanding their sources and degassing history (Newman et al., 1988; McIntosh et al., 2014; Castro et al., 2014).

This study focuses on oxygen analyses, since oxygen is a less exchangeable, labile element than hydrogen, allowing for less concern about long-term isotopic stability and preservation of primary values in older samples. For example, recent work by Nolan and Bindeman (2013) (see also D/H results in Cassel and Breecker, 2017) suggested that the hydrogen isotopic ratio of hydrated volcanic glass might shift in higher T experiments over time to equilibrate with surrounding waters, while the oxygen isotopic ratio does not change. We target rocks that have only primary magmatic water and those that have experienced secondary hydration by secondary environmental molecular water. Many of these are samples that we previously investigated for D/H and $H_2O_t$ (total water including $H_2O_m$ and $OH^-$) (Bindeman et al., 2012; Seligman et al., 2016; Martin et al., 2017). As there is a significant amount of new notation throughout this article, we include a list of commonly used notation and its associated definition in Table 1.The $\delta^{18}O$ of water in glasses that have been hydrated by typically low $\delta^{18}O$ and $\delta D$ surrounding meteoric water also contains important information about these hydrating waters. In particular, it is well understood that as climate fluctuates between warmer and colder temperatures the $\delta^{18}O$ and $\delta D$ values of precipitation change together along the meteoric water line (e.g. $\boldsymbol{\delta D = 8 \times \delta^{18}O + 10}$; Craig, 1961; Dansgaard, 1964). This shift in water isotopic ratios is also true for precipitation at higher versus lower latitudes, over topographic changes (Poage and Chamberlain, 2001), or farther into continental interiors versus near the coast (Dansgaard, 1964; Rozanski et al., 1993; Rowley et al., 2001; waterisotopes.org). Thus, the other goal of this study is to test the $\delta^{18}O$ of water in glass as a tool for paleoenvironmental studies.

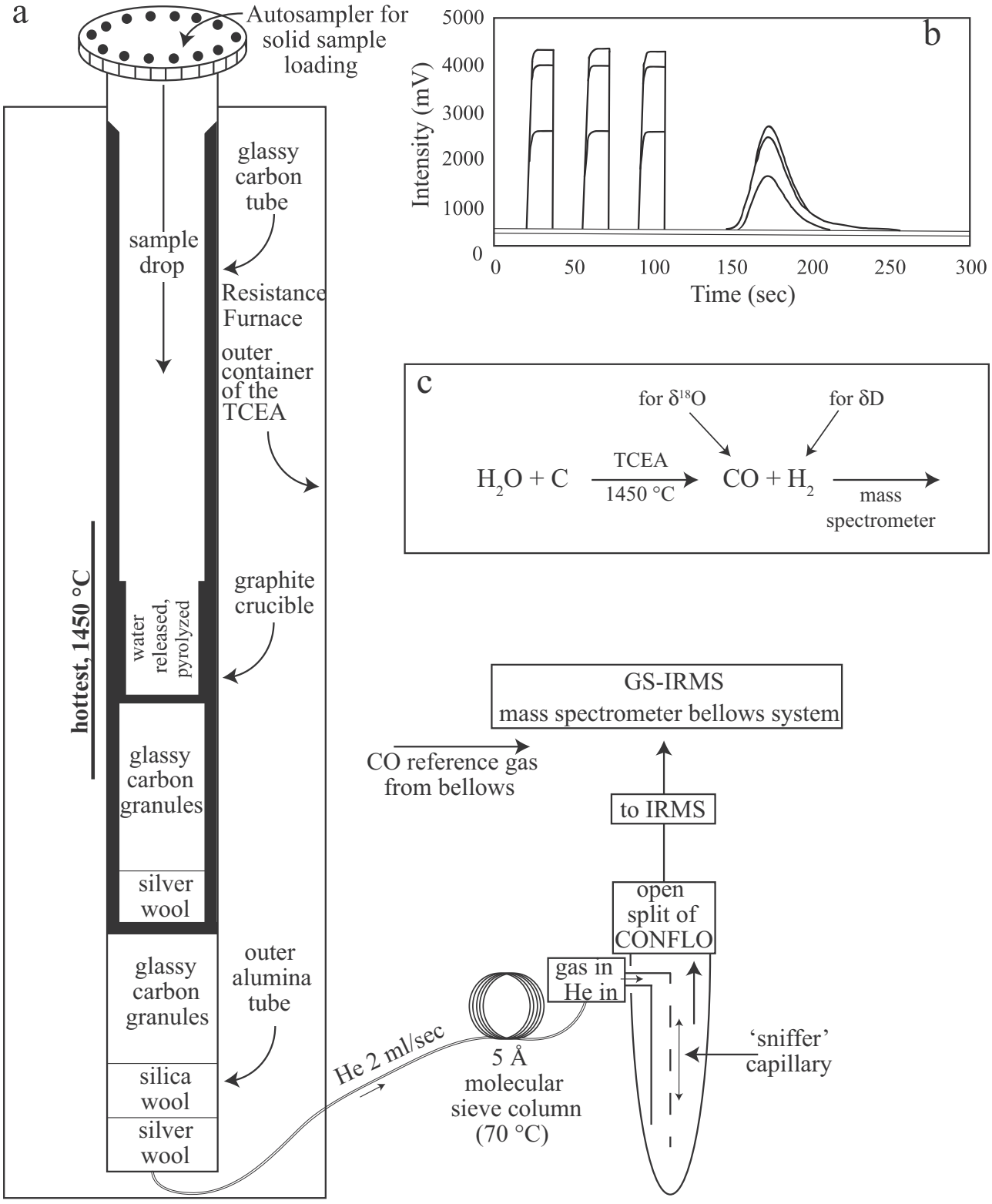


**Fig. 1.** The TCEA set up for oxygen and hydrogen isotopic analyses of glasses and phyllosilicates used in this study. a) Schematic of the TCEA Thermo-Scientific system, modified from Sharp et al., (2001). One at a time, samples or standards wrapped in silver foil are dropped into the glassy carbon reaction furnace held at 1450 °C, water is extracted and undergoes instantaneous pyrolysis into $H_2$ and CO gas in a He atmosphere. Gases are then passed through a 5 Å molecular sieve gas chromatographic column that separates the $H_2$ and CO gases and potential contaminants, through an open split, and into the mass spectrometer, where the reference gas is introduced from a separate cylinder or from the bellows system of the dual inlet. b) Example of CO pyrolysis analysis peaks of NBS30 mica with 3.5 wt% water, and three reference gas peaks (on-off, from bellows) matching intensities of the unknown. Comparable chromatogram will characterize D/H analyses of the $H_2$ portion of the gas, when run in the same or different analytical session. c) Water extraction and the high temperature pyrolysis reaction for oxygen isotope analyses on the TCEA.

**Table 1**
Definitions of notations used throughout the article.

| Notation | Definition |
|---|---|
| $OH^-$ | Hydroxyl water |
| $H_2O_m$ | Molecular water |
| $H_2O_t$ | Total water-in-glass (WIG) including hydroxyl and molecular |
| $\delta^{18}O_{BG}$ | The $\delta^{18}O$ value of the bulk glass |
| $\delta^{18}O_{TCEA}$ | The $\delta^{18}O$ of the total water that is analyzed by the TCEA ($H_2O_m$ and 1/2 of the $OH^-$) following standard correction |
| $\delta^{18}O_{RAW}$ | The raw $\delta^{18}O$ value given by the mass spectrometer prior to any correction |
| $\delta^{18}O_{\delta 13C\text{-}CORR}$ | The $\delta^{18}O_{TCEA}$ value following a $\delta^{13}C$ correction |
| $\delta^{18}O_{H2Om}$ | The $\delta^{18}O$ of the molecular water |
| $\delta^{18}O_{OH\rightarrow silicate}$ | The $\delta^{18}O$ of the oxygen from the hydroxyl that is left in the silicate during analysis |
| $\delta^{18}O_{OH\rightarrow H2Om}$ | The $\delta^{18}O$ of the $OH^-$ that is converted to $H_2O_m$ and analyzed by the TCEA |
| $\delta^{18}O_{Total}$ | The $\delta^{18}O$ of the total water (hydrogen-associated oxygen) present in a solid that contains both $OH^-$ and $H_2O_m$ prior to removal during analysis |
| $\delta^{18}O_{MET}$ | The $\delta^{18}O$ of the meteoric water, after a correction for pre-existing magmatic water |
| $10^3 ln\alpha_{silicate\text{-}H2Ot}$ | The oxygen isotope fractionation between the oxygen in the silicate and the hydrogen-bound oxygen, where $\alpha_{silicate\text{-}H2O} = (1000 + \delta^{18}O_{silicate}) / (1000 + \delta^{18}O_{H2O})$ |
| $10^3 ln\alpha_{rhyolite\text{-}H2O}$ | The oxygen isotope fractionation between the oxygen bound in the silicate and the hydrogen bound oxygen |
| $10^3 ln\alpha_{silicate\text{-}OH}$ | The oxygen isotope fractionation between the oxygen bound in the silicate and the hydroxyl bound oxygen |
| $\delta^{13}C_{analysis}$ | The $\delta^{13}C$ value of an individual analysis |
| $\delta^{13}C_{average}$ | The average $\delta^{13}C$ value for a specific run's analyses |

## 2. Methods

We focus on two primary types of glasses in this study, including both primary magmatic and secondary meteoric glasses. First, we utilized rapidly quenched and degassed basaltic to rhyolitic volcanic glasses containing only <0.6 wt% primary magmatic water and thus a high $OH^-$ to $H_2O_m$ ratio (Ihinger et al., 1999) to understand the $\delta^{18}O$ values of the hydroxyl (Fig. 2). Natural samples come from Volcán de Fuego (1974 CE eruption), Mt. Spurr (1992 CE), and the 7.7 ka Cleetwood rhyolite from Mt. Mazama. In addition, we analyze synthetically hydrated dacite (D2) glass from Bindeman et al. (2012) that was experimentally melted and hydrated at 900 °C with water from Fiji ($\delta D = -41.8‰$, $\delta^{18}O = -5.3‰$) for 1 h. Here, the isotopic ratio of the bulk water, $OH^-$ to $H_2O_m$ water speciation, and the temperature of hydration are known. We also analyzed a hydrous rhyolitic glass from the Iceland Deep Drilling Project that was quenched almost instantaneously with 1.77 wt% water at a depth of approximately 2.1 km after being intercepted by a drill core. We present new isotopic results for this material that was described in detail by Zierenberg et al. (2012) and further analyzed by Bindeman and Lowenstern (2016). The relative proportions of $H_2O_m$ and $OH^-$, and the observed 930 °C quench temperature are known for this sample (Table 2).

The second group of samples that we analyze in this work for the $\delta^{18}O$ of the hydroxyl-bound oxygen include glasses that were secondarily hydrated by environmental meteoric waters: 7.7 ka Mt. Mazama from Nolan and Bindeman (2013), 631 ka Lava Creek Tuff from Bindeman et al. (2007), and 8 ka Hrafntinnusker eruption from Martin et al. (2017) (Table 3). The latter glasses from Hraftinnusker were secondarily hydrated at elevated temperature (likely >150 °C) shortly after eruption, as were the Yellowstone perlites from the Bindeman and Lowenstern (2016) study.

Tephra samples were lightly disaggregated and sonicated for 60 min to remove the finest particles and clays (if any). Glass particles were then dried, examined under a microscope, and 2–12 mg of the freshest glass concentrate smaller than 0.5 mm in the longest direction and free of minerals were packaged in silver foil. Average glass wall thickness of the studied materials was no >25 μm (Seligman et al., 2016). Prior to analysis, all samples were heated in a vacuum-sealed oven 12–18 h or overnight at 130 °C to remove any atmospheric moisture and then loaded and purged with He carrier gas in a Costech zero-blank autosampler. Martin et al. (2017) present more details on the size fraction analysis and reproducibility of different glasses and micas. Seligman et al. (2016) and Dettinger and Quade (2015) additionally describe the advantages of not treating samples in 8% HF solution prior to analysis.

Samples for TCEA analyses using the CO method (Fig. 1) were prepared and treated similar to those for hydrogen isotope analyses (e.g. Bindeman et al., 2012; Martin et al., 2017). Milligram quantities of sample were dropped one at a time into the reduction furnace (Fig. 1) and almost instantaneously heated to 1450 °C, allowing water to be released off the solid and instantaneously converted to CO gas through high temperature reduction with the surrounding glassy carbon (e.g. Brand et al., 1994; Sharp et al., 2001). Following rapid heating, the CO gas was then passed through a 0.6 m long, short packed, 5 Å molecular sieve column, and then through an open split and into the mass spectrometer. Analyses of the CO gas are conducted relative to a reference gas from the University of Ottawa G.G. Hatch Stable Isotope Laboratory with a known $\delta^{18}O$ value of −5.5‰ relative to VSMOW (Vienna Standard Mean Ocean Water), which is introduced from the bellows system of a dual inlet continuous flow run method (Fig. 1). Calibration of the final value is performed using solid and liquid standards with known $\delta^{18}O$ values (see below). These methods are described in detail in the Appendix.

## 3. Results

### 3.1. Testing the viability of extracting hydrogen-bound oxygen using the TCEA

It is important to check if the $\delta^{18}O$ values of water extracted at 1450 °C from silicates is not shifted towards the silicate $\delta^{18}O$ value upon extraction, and to verify that the extracted $\delta^{18}O$ values reflect those of the original hydrogen-bound oxygen. We thus first performed a series of tests involving anhydrous and minimally hydrous silicates and oxides. First, we loaded our GISP (−24.8‰) water standards that are already welded inside Ag cups inside of another Ag cup loaded with 3–4 mg of Cleetwood rhyolite (0.2 wt% magmatic $H_2O$ with $\delta^{18}O_{Total} = -1.5‰$, Seligman et al., 2016, new data in this work, Fig. 3). This tests the possibility and extent of exchange between the +7‰ bulk silicate volcanic glass with the isotopically very light −24.8‰ water at 1450 °C inside the graphite crucible. We observe that the $\delta^{18}O$ values of extracted water return slightly heavier values than the $\delta^{18}O$ values of the GISP standards run without the Cleetwood rhyolite. However, if we correct for the 0.2 wt% residual water from the Cleetwood rhyolite, the raw $\delta^{18}O$ values come closer to the GISP analyses (within 0.9‰) from that same session, indicating <3% silicate-water exchange during extraction. Similar experimentation done with anhydrous rhyolite/basalt and GISP by Bindeman and Lowenstern (2016) yielded a positive 0.53‰ shift for rhyolite and a negative 0.26‰ shift for basalt, within the error of the measurements (Fig. 3). These tests demonstrate limited (~1‰) exchange between silicate and water during the approximately 3 min extraction and pyrolysis at 1450 °C in the TCEA system.

#### 3.1.1. Extracting oxygen from nominally anhydrous silicates

Next, to check if anhydrous silicates and Fe-oxides pyrolyze in a glassy carbon tube and release CO gas we performed a series of tests. First, we analyzed individual components of silicate melt: a range of synthetic albite-anorthite feldspar glasses ($Ab_{50}$, $Ab_{75}$, $Ab_{100}$), quartz from the Bishop tuff, UOG garnet, San Carlos olivine, and a series of Fe-silicate glasses (Fig. 4). The majority of these silicates produce peaks below our typical background range. However, our analysis of 5.7 mg of UOG garnet produced a slightly higher peak than the other silicates, which is likely due to the presence of FeO and $Fe_2O_3$, or the

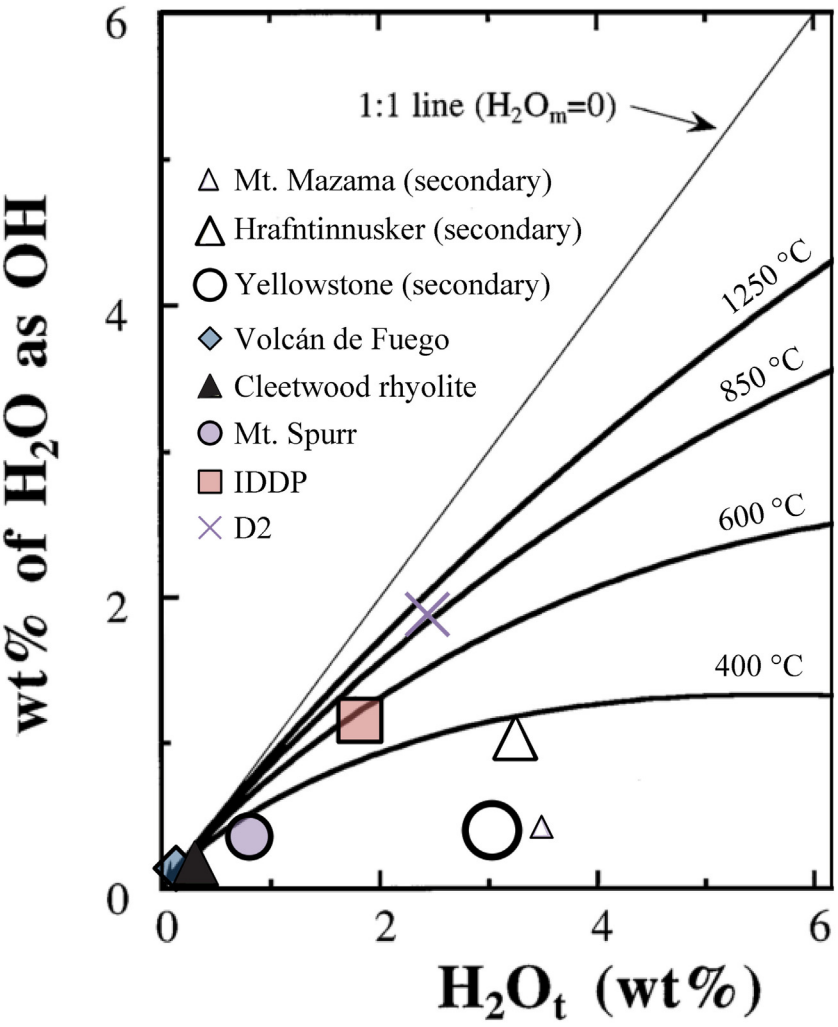


**Fig. 2.** Equilibrium partitioning of $H_2O_t$ and $OH^-$ as a function of total water in rhyolitic glasses and melts (modified from Ihinger et al., 1999), illustrating the larger relative quantities of $OH^-$ at higher temperatures in contrast to the larger quantities of $H_2O_m$ at lower temperatures. Magmatic glasses studied here with determined or estimated relative quantities of $OH^-$ and $H_2O_m$ are plotted (data from this study; Nolan and Bindeman, 2013; Bindeman and Lowenstern, 2016; Martin et al., 2017). Note the larger relative proportions of $H_2O_m$ in the secondarily hydrated glasses (open symbols).

100–1000s of ppm of water in this nominally anhydrous phase, as was also noted by Gong et al. (2008) for other metamorphic garnets.

Second, we ran milligram quantities of pure, nominally anhydrous FeO and $Fe_3O_4$ powders to test for the production of CO related to the iron reduction reactions $Fe_3O_4 + C = 3FeO + CO$ and $FeO + C = Fe + CO$. Results show the appearance of irregular peaks (Fig. 4). FeO produced singular large peaks, while $Fe_3O_4$ produced very broad peaks, suggesting the reduction is not instantaneous and takes a long time, worsening the background for subsequent analyses. However, when oxides are fused together into silicates to form fused FeO-$SiO_2$ glasses

**Table 2**
Data and location information from isotopic analyses of volcanic glasses and phyllosilicates that have been standard corrected. All δ values are in per mil (‰) deviations.

| Sample name | Source | Date analyzed | n | $\delta^{13}C$ (‰) | $\delta^{18}O_{BG}$ (‰) | $\delta^{18}O_{RAW}$ (‰) | $\delta^{18}O_{TCEA}$ (‰) | 1 s.d. | $\delta^{18}O_{H2Om}$ (‰) | 1 s.d. | $\delta^{18}O_{OH}$ (‰) | 1 s.d. | $\delta^{18}O_{Total}$ (‰) | 1 s.d. |
|---|---|---|---|---|---|---|---|---|---|---|---|---|---|---|
| Cleetwood | Mt. Mazama: Cleetwood rhyolite | 1/7/16 Carousel #2 | 2 | −25.16 | 6.7 | −8.7 | −8.9 | 1.2 | 6.6 | 0.2 | −1.9 | 0.4 | −1.5 | 2.1 |
| IDDP | Iceland: Krafla rhyolite | 1/7/16 Carousel #1 + 2 | 3 | −25.27 | 3.1 | −11.4 | −11.5 | 0.4 | 3.0 | 0.2 | −11.5 | 0.5 | −6.6 | 0.4 |
| D2 | Kamchatka: synthetic dacite[a] | 22/04/2013 | 3 | −25.26 | 5.0 | −7.7 | −5.6 | 0.6 | 5.3 | 0.2 | −2.7 | 1.2 | −1.2 | 0.9 |
| VF-74-45 | Volcán de Fuego: 1974 basalt | 22/04/2013 | 3 | −25.48 | 6.3 | −3.6 | −1.5 | 0.7 | 7.3 | 0.2 | 3.6 | 1.2 | 3.7 | 5.0 |
| 42-Cordova | Mt. Spurr: 1992 dacite | 4/4/2013 | 3 | −25.09 | 6.2 | −1.9 | −2.2 | 1.5 | 6.8 | 0.2 | 0.8 | 0.5 | 1.6 | 0.8 |
| 57-Ashton | Mt. Spurr: 1992 dacite | 4/4/2013 | 3 | −25.35 | 6.2 | −3.8 | −4.1 | 1.0 | 6.8 | 0.2 | −0.5 | 2.7 | 0.5 | 1.1 |
| BUD | Butte (MT): biotite standard | 2014–2016 | 37 | −24.68 | 5.1 | −5.4 | −5.6 | 1.0 | NA | – | 0.6 | 0.8 | NA | – |
| NBS30 | California batholith: biotite standard | 2014-2016 | 24 | −24.60 | 5.1 | −3.3 | −5.3 | 2.4 | NA | – | 0.9 | 2.5 | NA | – |
| RUH | Russia: muscovite standard | 2014–2016 | 13 | −24.37 | 7.4 | −7.5 | −5.0 | 2.3 | NA | – | 1.7 | 2.4 | NA | – |
| Kaolinite | Sigma-Aldrich: kaolinite powder | 8/13/14 6/9/16 | 3 | −24.64 | 16.3 | 7.3 | 11.2 | 3.1 | NA | – | 10.9 | 0.1 | NA | – |
| Brucite | Austria: Lobminggraben | 8/13/14 6/9/16 | 10 | −22.87 | 5.2 | 2.9 | 8.7 | 1.9 | NA | – | 5.1 | 0.2 O | NA | – |

[a]Experimentally synthesized glasses from Bindeman et al. (2012)

$\delta^{18}O_{BG}$ = the $\delta^{18}O$ value of the bulk glass; $\delta^{18}O_{RAW}$ = the raw $\delta^{18}O$ value given by the mass spectrometer prior to any correction; $\delta^{18}O_{TCEA}$ = the $\delta^{18}O$ value given by the mass spectrometer following standard correction; $\delta^{18}O_{H2Om}$ = the $\delta^{18}O$ value of the molecular water; $\delta^{18}O_{OH}$ = the $\delta^{18}O$ of the hydroxyl; $\delta^{18}O_{Total}$ = the $\delta^{18}O$ value of the total water.

**Table 3**
Data and location information from oxygen isotopic analyses of felsic volcanic glasses that have been hydrated by meteoric waters that have been standard corrected. All δ values are in per mil (‰) deviations.

| Sample name | Source | Date analyzed | n | $\delta^{13}C$ (‰) | $\delta^{18}O_{BG}$ (‰) | $\delta^{18}O_{RAW}$ (‰) | $\delta^{18}O_{TCEA}$ (‰) | 1 s.d. | $H_2O_t$ (wt %) | $\frac{SiOH}{H_2O_m}$ | $\delta^{18}O_{Total}$ (‰) | 1 s.d. | Temperature of hydration used (°C) |
|---|---|---|---|---|---|---|---|---|---|---|---|---|---|
| Mazama[a] | Mt. Mazama: (7.7 ka) | 1/7/16 Carousel #1 | 10 | −25.57 | 6.4 | 1.1 | −7.1 | 0.8 | 2.90 | 0.5 | −5.3 | 0.4 | 25 |
| IB01-2[b] | Lava Creek Tuff: (630 ka) | 4/4/2013 | 1 | −24.94 | 6.5 | −0.2 | 5.9 | – | 2.26 | – | – | – | – |
| IB01-3[c] | Lava Creek Tuff: (630 ka) | 4/4/2013 | 3 | −25.38 | 6.5 | −1.9 | 4.5 | 0.42 | 1.94 | – | – | – | – |
| IB04-3[c] | Lava Creek Tuff: (630 ka) | 4/4/2013 | 1 | −24.85 | 6.5 | 1.7 | 7.8 | 0.35 | – | – | – | – | – |
| IB01-1[d] | Lava Creek Tuff: (630 ka) | 4/4/2013 | 3 | −25.38 | 6.5 | −1.7 | 4.6 | 0.19 | 2.15 | – | – | – | – |
| IB01-5[e] | Lava Creek Tuff: (630 ka) | 4/22/2013 | 3 | −25.22 | 6.5 | −6.0 | 2.3 | 0.17 | 1.74 | – | – | – | – |
| HSK1[f] | Hrafntinnusker: (8 ka Iceland) | 4/20/2013 | 2 | −25.12 | 3.9 | −6.3 | 2.4 | 1.01 | 5.50 | 0.4 | −2.4 | 0.4 | 150 |
| HSK3[f] | Hrafntinnusker: (8 ka Iceland) | 4/19/2013 | 1 | −26.20 | 3.9 | −6.3 | 3.5 | – | 4.70 | 0.4 | −3.1 | 0.4 | 150 |
| HSK4[f] | Hrafntinnusker: (8 ka Iceland) | 4/19/2013 | 2 | −25.17 | 3.9 | −9.3 | −1.1 | 0.41 | 3.60 | 0.3 | −6.0 | 0.5 | 150 |
| HSK7[f] | Hrafntinnusker: (8 ka Iceland) | 4/19/2013 | 3 | −24.86 | 3.9 | −7.6 | −0.3 | 0.17 | 3.50 | 0.2 | −4.6 | 0.6 | 150 |

[a]Experimentally synthesized glasses from Bindeman et al. (2012).
$\delta^{18}O_{BG}$ = the $\delta^{18}O$ value of the bulk glass; $\delta^{18}O_{RAW}$ = the raw $\delta^{18}O$ value given by the mass spectrometer prior to any correction; $\delta^{18}O_{TCEA}$ = the $\delta^{18}O$ value given by the mass spectrometer following standard correction; $\delta^{18}O_{H2Om}$ = the $\delta^{18}O$ value of the molecular water; $\delta^{18}O_{OH}$ = the $\delta^{18}O$ of the hydroxyl; $\delta^{18}O_{Total}$ = the $\delta^{18}O$ value of the total water.
[a] Data from Nolan and Bindeman, 2013. [b–e] from Bindeman et al. (2007);
[b] Collected in Springtown, NE.
[c] Collected in Iowa.
[d] Collected in Springtown, NE.
[e] Collected in South Dakota.
[f] From Martin et al. (2017).

with variable proportions of Fe and Si, the CO production is severely reduced to background levels (Fig. 4). Third, when biotite mica standards (Fe-bearing BUD and NBS30) are compared to our muscovite mica standard (RUH) we observe no trend in terms of Fe-bearing micas having larger (or smaller) errors relative to Fe-free muscovite.

### 3.1.2. Correcting versus not correcting for potential kinetic isotope fractionation

A common practice in stable isotope analyses using the CO molecule is to ignore the $\delta^{13}C$ values of the carbon crucible, glassy carbon granules, and the reactor, and to correct the resulting $\delta^{18}O$ values only by concurrently run standards with known $\delta^{18}O$ values (Sharp et al., 2001). We explored this procedure further by processing all of our data with and without a correction for variations in their $\delta^{13}C$ values. These $\delta^{13}C$ values should theoretically stay constant in the same analytical session, because mass dependent isotope fractionation of $^{18}O/^{16}O$ ratios is expected to be 2× that of $^{13}C/^{12}C$ ratios in any mass dependent kinetic process. Several subsequent data figures and tables in the main text have a correlating figure and table that has been $\delta^{13}C$ corrected in the Appendix. After performing these two separate corrections, we

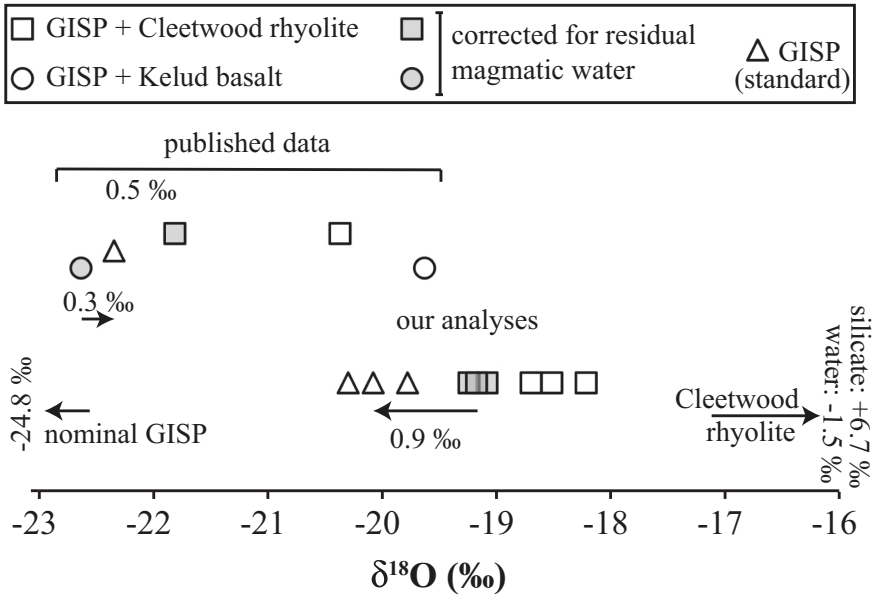


**Fig. 3.** Results of tests to determine the magnitude of interaction between silicate and waters during water extraction and pyrolysis to CO in the TCEA. Data are from Cleetwood rhyolite and Kelud basalt ($\delta^{18}O$ 6.7‰ and 5.8‰) containing 0.2 wt% and 0.1 wt% of magmatic water, respectively, loaded together with isotopically very negative GISP (−24.8‰, Greenland Ice Sheet Precipitation) water packets. This test demonstrates that there is an approximately 1‰ shift (or <4% difference) between the raw $\delta^{18}O$ value of GISP run during the same session as the GISP analyzed together with these glasses. The isotopic shift is expected to be less for a smaller difference between the $\delta^{18}O$ of the glass and the $\delta^{18}O$ of the surrounding waters. Also included are published data from Bindeman and Lowenstern (2016) for similar tests in a different analytical session using rhyolite and basaltic glass with GISP water packets that also show no significant per mil deviations. GISP values are a few per mil different from nominal due to instrumental mass fractionations (see Fig. 1 and text for details).

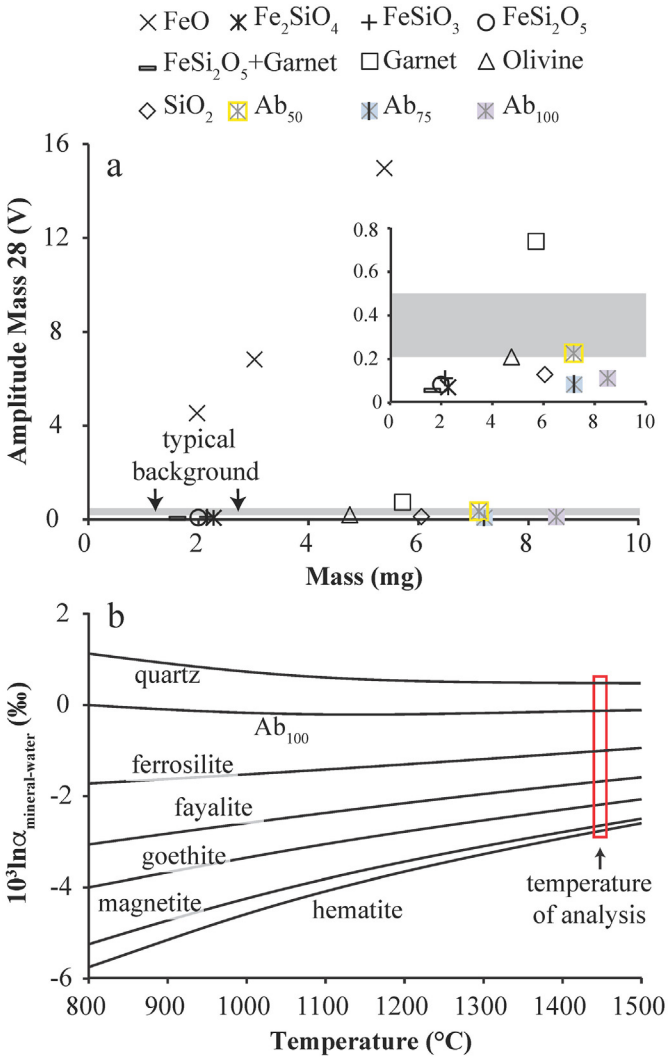


**Fig. 4.** Contributions of anhydrous oxide and mineral compositions to CO backgrounds (grey bar). Results of a test to determine whether anhydrous feldspar glasses, quartz, garnet, olivine, FeO and $Fe_3O_4$, oxides, or Fe-silicate glasses pyrolyze and release CO during the 1450 °C TCEA analyses. a) Powdered anhydrous FeO reacts with carbon in the TCEA crucible, yielding a proportional increase in yield (likely partial reduction to iron), while silicate glasses or minerals, including Fe-silicates have significantly smaller yields, not exceeding typical Fe-free backgrounds. b) $10^3 ln\alpha_{mineral\text{-}water}$ values (Zheng, 1991, 1993a, 1993b, 1998) show the expected fractionation ranging from approximately −3 to +1‰ at 1450 °C. This test illustrates almost no fractionation at 1450 °C; isotopic values from silicate-derived oxygen are expected to be close to the bulk value at the 1450 °C extraction (see Section 3.1 for discussion).

compared the pooled standard deviations for each group of samples (water standards, micas, unknowns containing only $OH^-$, and unknowns containing $OH^-$ and $H_2O_m$), but there is no consistent difference between the two methods of sample correction (Table A5). Although it is important to monitor the $\delta^{13}C$ values for outliers, it is not clear that a $\delta^{13}C$ correction adds benefit. This may also indicate that continuous flow transfer of CO to the mass spectrometer may not undergo kinetic isotope fractionation since it is carried by helium carrier gas. Alternatively, a multi-step process of chromatography, gas transfer and the open split has mutually compensating effects that masks kinetic isotope fractionation.

### 3.2. $\delta^{18}O$ of quenched magmatic water within silicate glass and mica

#### 3.2.1. High temperature IDDP glass as an example for calculations

Volcanic glass has a mixture of $H_2O_m$ and $OH^-$ in either known or expected proportions based on their high temperature speciation (Fig. 2) (Ihinger et al., 1999; Newman and Lowenstern, 2002). The CO analysis on the TCEA reports a bulk $\delta^{18}O$ for water extracted from a solid ($H_2O_m$ and $OH^-$), but records only half the oxygen of the $OH^-$ present in the silicate ($\boldsymbol{2OH^- \rightarrow H_2O + O_{silicate}^{2-}}$). It is, however, possible to resolve this using mass balance relationships, and by employing two primary assumptions about the associated temperature-dependent equilibrium fractionations: 1) the water present as $H_2O_m$ has a $10^3 ln\alpha_{silicate\text{-}H2Om}$ that can be computed based on equilibrium fractionation using the known chemical composition of the melt and the temperature at which the melt was quenched (e.g. Zheng, 1991; Zheng, 1993a; Zhao and Zheng, 2003) and 2) the half of the hydroxyl-sourced-oxygen left in the silicate has an equilibrium fractionation between the silicate oxygen and the oxygen that is released, which can be calculated given the known composition of the silicate and the temperature of extraction (1450 °C). Since the reaction during analysis should take place only within the reaction crucible, and occurs rapidly, we assume this to be an equilibrium fractionation, and not a kinetic fractionation. We also see evidence in our analyses for this being an equilibrium fractionation, in the relatively heavy $\delta^{18}O_{H2Om}$ values that are based on equilibrium with the host silicate and the light $\delta^{18}O_{TCEA}$ (the $\delta^{18}O$ value determined by the TCEA following standard correction) values that we measure. Utilizing these assumptions, we can use mass balance to determine the $\delta^{18}O$ of the total water in the glass.

We thus analyzed hydrous volcanic glass quenched at high temperature with a range of known $H_2O_m$ and $OH^-$ concentrations (Figs. 2, 5; Table 2). We utilize the IDDP glass here as an example of how all the high temperature glasses were processed. The IDDP rhyolite has known relative $H_2O_m$ and $OH^-$ concentrations that were measured by FTIR, a known chemical composition, and a known melt quench temperature of 885 °C (Zierenberg et al., 2012). The computed $10^3 ln\alpha_{rhyolite\text{-}H2Om}$ from Zhao and Zheng (2003) at this temperature is 0.1‰. Given the bulk silicate $\delta^{18}O$ of 3.1‰, the $\delta^{18}O$ of the molecular water in glass ($\delta^{18}O_{H2Om}$) is 3.0‰.

Similarly, to determine the $\delta^{18}O_{OH\rightarrow silicate}$, we use the same steps to calculate the fractionation between the rhyolite glass and the half of the oxygen from the $OH^-$. In this case, we use a high extraction temperature of 1450 °C, at which, the $10^3 ln\alpha_{rhyolite\text{-}H2Om} = \delta^{18}O_{H2O} - \delta^{18}O_{silicate} = 0.0‰$, so the water that is left in the silicate at 1450 °C is assumed to be the same $\delta^{18}O$ as the bulk silicate (3.1‰). The isotope fractionation associated with water extraction from the $OH^-$ groups ($\boldsymbol{2OH^- = H_2O_m}$

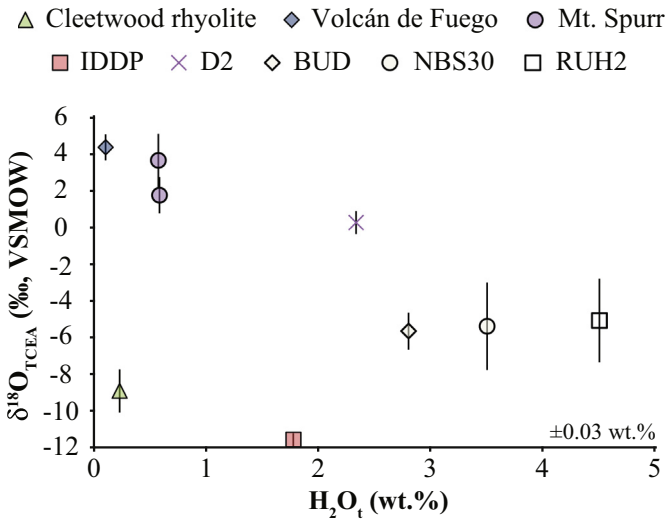


**Fig. 5.** $\delta^{18}O_{TCEA}$ values of water extracted from magmatic glasses and micas relative to the $H_2O_t$ (wt%) of the glass. Values here have been standard-corrected to the VSMOW scale, but have not been corrected for the half of the oxygen initially contained as $OH^-$ ($2OH^- = H_2O_m + O_{silicate}^{2-}$) and remains in the silicate during thermal extraction. Error bars for the $\delta^{18}O_{TCEA}$ values represent 1 s.d. for repeat analyses. The reproducibility of our wt% $H_2O_t$ analyses is ±0.03 wt%.

$+ O_{silicate}^{2-}$) is calculated to determine the $\delta^{18}O_{OH\rightarrow H2Om}$ analyzed by the TCEA. The $\delta^{18}O_{OH\rightarrow H2Om}$ can now be computed based on known mass balance relationships. We already know that:

$$(F_{H_2O_m} + F_{OH\rightarrow H_2O_m}) \times \delta^{18}O_{TCEA} = F_{H_2O_m} \times \delta^{18}O_{H_2O_m} + F_{OH\rightarrow H_2O_m} \times \delta^{18}O_{OH\rightarrow H_2O_m} \quad (1)$$

where $\delta^{18}O_{TCEA}$ is the $\delta^{18}O$ of the total water that is analyzed by the TCEA ($H_2O_m$ and 1/2 of the $OH^-$), $F_{H2Om}$ and $\delta^{18}O_{H2Om}$ are the fraction and the isotopic ratio of the molecular water respectively, $F_{OH\rightarrow H2Om}$ is the fraction of the total water that is present as $OH^-$ and converted to $H_2O_m$ during analysis (half of the total $OH^-$), and $\delta^{18}O_{OH\rightarrow H2Om}$ is the $\delta^{18}O$ of the 1/2 of the $OH^-$ that is extracted from the glass and contributes to the total water analyzed by the TCEA. The latter parameter is:

$$\delta^{18}O_{OH\rightarrow H_2O_m} = \frac{(F_{H_2O_m} + F_{OH\rightarrow H_2O_m}) \times \delta^{18}O_{TCEA} - F_{H_2O_m} \times \delta^{18}O_{H_2O_m}}{F_{OH\rightarrow H_2O_m}} \quad (2)$$

Using these relationships for the IDDP glass, the equilibrium value of $\delta^{18}O_{H2Om}$ (3.0‰), and the mass balance of Eq. (1), we can predict that the total $\delta^{18}O$ of the $OH^-$ present in the IDDP volcanic glass is −11.5‰ [0.46 s.d.] (Fig. 6).

We also calculate the $\delta^{18}O$ of the $\delta^{18}O_{Total}$ of the total water present, using the following mass balance relationship:

$$(F_{H_2O_m} + F_{OH^-}) \times \delta^{18}O_{Total} = (F_{H_2O_m}) \times \delta^{18}O_{H_2O_m} + (F_{OH^-}) \times \delta^{18}O_{OH^-} \quad (3)$$

where $F_{OH^-}$ and $\delta^{18}O_{OH-}$ are the fraction and isotopic values of the water present as $OH^-$, and $F_{OH^-} + F_{H2Om} = 1$. Using the last relationship, we determine a $\delta^{18}O_{Total}$ for IDDP of −6.6‰ [0.35 s.d.] (Fig. 7). This is the value of all hydrogen-associated water in the IDDP glass.

### 3.2.2. Extraction of water from mica

This same mass balance as in Eqs. (2)–(3) can be utilized for micas that contain water only as $OH^-$. Here the mass balance is much simpler, because there is no $H_2O_m$. As $10^3\ln\alpha_{silicate\text{-}OH}$ internal fractionations increase with decreasing temperature (Zheng, 1993a), we assume the temperature to be similar to the diffusional closure temperature for the plutonic and hydrothermal mica standards used in our study (200–500 °C; Eiler et al., 1992). However, the fractionation that matters most for our calculations is the high temperature extraction reaction at 1450 °C.

For conventional simplicity and comparison with previous studies, we assume that the bulk $\delta^{18}O$ value of the mica silicate can be taken as a proxy of the anhydrous silicate. If we take BUD mica standard as an example (Table 2), the $\delta^{18}O_{TCEA}$ of the extracted water value is −5.6‰ [0.74 s.d.], which is sourced from a bulk $\delta^{18}O$ mica value of 5.1‰ [0.1 s.d.]. At 1450 °C biotite has a $10^3\ln\alpha_{silicate\text{-}OH}$ of −1.3‰ (Zheng, 1993a), which is a larger fractionation than the rhyolite above due to the lower silica bulk chemical compositions. Thus, the $\delta^{18}O_{OH\rightarrow silicate}$ value is +6.4‰ [0.22 s.d.], making the residual mica negligibly heavier (likely up to 0.02‰) than the starting mica. The $\delta^{18}O_{Total}$ for water (total $OH^-$) extracted from micas is:

$$\delta^{18}O_{Total} = \frac{1}{2}\left(\delta^{18}O_{TCEA}\right) + \frac{1}{2}\left(\delta^{18}O_{OH\rightarrow silicate}\right) \quad (4)$$

Note that for a theoretically more accurate treatment one should utilize the absolute ratio of $^{18}O/^{16}O$, and recompute the deltas after the algebraic manipulations in Eqs. (1)–(4). The computed deltas will be ~0.1‰ different than those computed in the above equations, which is well within the errors of these calculations. Our mica mass balance demonstrates that, similar to glasses, the $\delta^{18}O_{Total}$ of the water in the micas is 6–7‰ heavier than the extracted water $\delta^{18}O_{TCEA}$ value

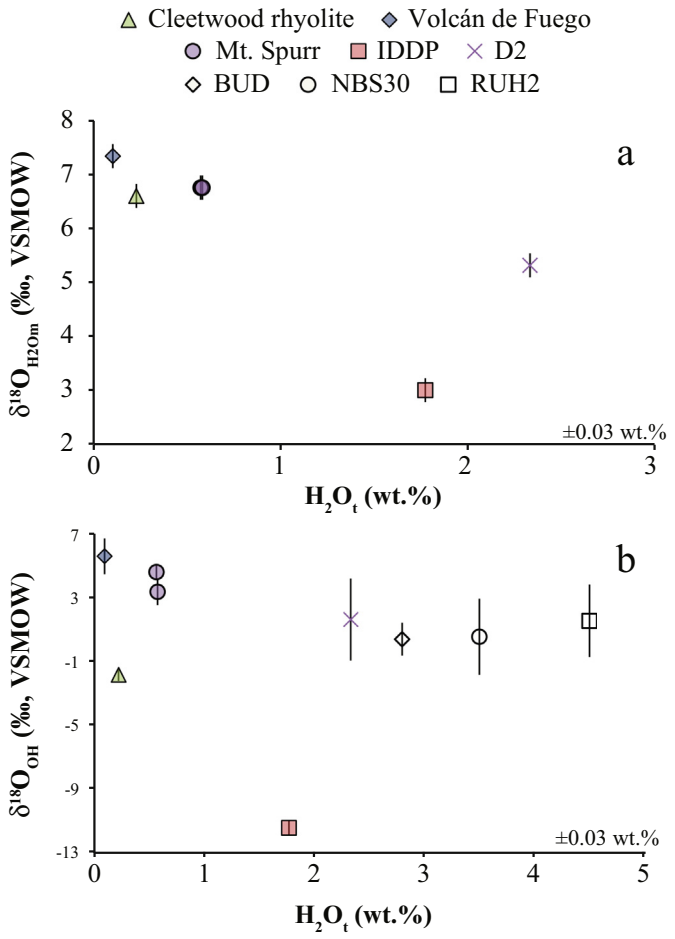


**Fig. 6.** Calculated $\delta^{18}O$ values of water in magmatic glasses and micas based on relative proportions of $H_2O_m$ and $OH^-$ in silicates, in relation to total water concentration (from Fig. 2). a) $\delta^{18}O_{H2Om}$ in relation to the total water concentration. $\delta^{18}O_{H2Om}$ values were calculated based on published $10^3\ln\alpha$ values between water and the silicate (Zheng, 1991, 1993a, 1993b; Zhao and Zheng, 2003); see text for discussion. b) $\delta^{18}O_{OH}$ values; calculated based on Eq. (2) and known $10^3\ln\alpha$ values at the 1450 °C temperature of extraction. Error bars are 1 s.d. based on simple error propagation described in the Appendix.

(Fig. 5). This computed $\delta^{18}O_{Total}$ depends on the quantity of $OH^-$ and the $\delta^{18}O$ of the bulk silicate. Therefore, by mass balance, the oxygen left in the silicate during extraction has a $\delta^{18}O$ value that is 0.8 to 1.3‰ heavier than the bulk silicate $\delta^{18}O$ value.

The $\delta^{18}O$ values of the total water extracted from BUD and NBS30 biotite, and RUH muscovite show a similar trend in $\delta^{18}O_{OH}$ values (Table 2; Figs. 5–6). Since only half the $OH^-$ is extracted, and the heavier half is left behind in the silicate, the $\delta^{18}O_{TCEA}$ values (−5.2 to −4.7‰) are lighter than the $\delta^{18}O_{Total}$ values (0.4 to 1.6‰).

### 3.2.3. Silicate glasses

Here, we report observed trends of $\delta^{18}O$ of magmatic water extracted from natural, rapidly quenched mafic and silicic volcanic glass (Table 2; Figs. 5–7). In many cases, the relative quantities of $OH^-$ and $H_2O_m$ had not been determined prior to $\delta^{18}O$ analyses by FTIR. Instead we used VoltileCalc (Newman and Lowenstern, 2002) (Table 4) at the known or estimated magmatic temperature (e.g. Fig. 2) for these rapidly quenched magmatic samples. When comparing Fig. 5 ($\delta^{18}O_{TCEA}$) to Fig. 7 ($\delta^{18}O_{Total}$), the primary distinction is a trend towards heavier $\delta^{18}O_{Total}$ values (−6.6 to +5.8‰) relative to the lighter $\delta^{18}O_{TCEA}$ values (−11.5 to +4.4‰). This is due to disproportionation in which light oxygen is extracted along with the $H_2O_m$, as discussed above.

Plotted differently, there is a negative trend between magmatic temperatures and the $10^3\ln\alpha_{silicate\text{-}H2Ot}$ for all silicates in this study (Fig. 9).

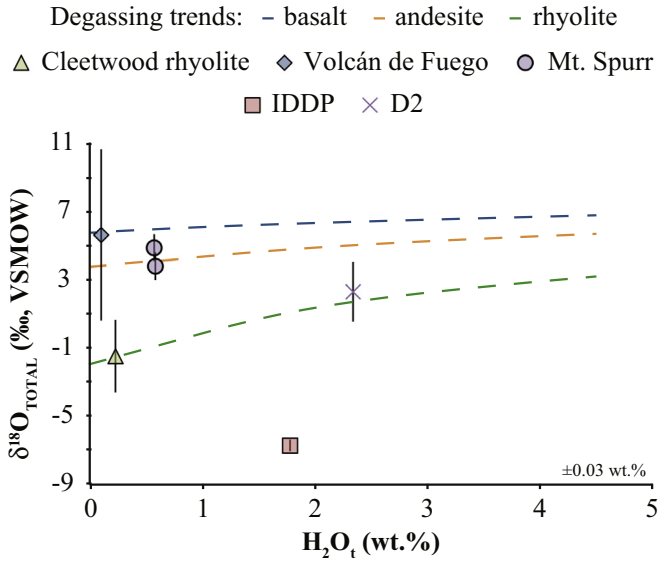


**Fig. 7.** $\delta^{18}O_{Total}$ values of water extracted from hydrous glasses relative to the $H_2O_t$ (wt%) of the glass. These values represent the total $\delta^{18}O$ of the hydrogen-bound oxygen in glass ($H_2O_m$ and $OH^-$) present in it prior to analysis. Note the shift in $\delta^{18}O$ values following the total water correction to more positive $\delta^{18}O$ values in comparison to Fig. 5, which is based on the relative quantities of $OH^-$ in the glass and the $\delta^{18}O$ of the glass. Also included are calculated $\delta^{18}O$ volcanic degassing trends for basalt, andesite, and rhyolite starting from a normal bulk magma $\delta^{18}O$ value of 6.5‰. No volcanic degassing trend is included for IDDP or D2, since both glasses are water undersaturated and contain bubbles. Error bars are 1 s.d. based on simple error propagation described in the Appendix.

The highest temperature glass (Volcán de Fuego) has the smallest $10^3\ln\alpha_{silicate\text{-}H2Ot}$ (0.7‰ [0.89 s.d.]) and the lowest temperature glass (IDDP) has the largest $10^3\ln\alpha_{silicate\text{-}H2Ot}$ (9.8‰ [0.06 s.d.]). Similar trends of decreasing $10^3\ln\alpha$ values for the silicate-OH and silicate-$H_2O_m$ are also shown in Fig. 9 for all glasses in this study.

Two of our magmatic glasses (IDDP and D2) are water undersaturated and do not follow the same magmatic trends as the <1 wt% water magmatic glasses. The IDDP glass is from the Krafla geothermal field, where the geothermal fluids primarily consist of low δD and $\delta^{18}O$ meteoric waters ($\delta^{18}O = -12.5$‰, $\delta D = -90$‰) (Sveinbjörnsdóttir et al., 1986) and the hydrothermally altered rocks sourced from the Krafla geothermal field have $\delta^{18}O_{BG}$ values as low as −11. The low $\delta^{18}O_{Total}$ value of the IDDP glass, relative to the other magmatic glasses, may be sourced from the surrounding low $\delta^{18}O$ source rock and waters; some of which may be contained in the 5–7% vapor bubbles in the analyzed IDDP glass. The D2 glass was synthesized at 900 °C from powdered rock with Fiji water ($\delta D = -41.8$‰, $\delta^{18}O = -5.3$‰) in a study by Bindeman et al. (2012). Unlike the IDDP glass, the data for the 1 h long synthesis experiment agrees more closely with the $\delta^{18}O_{H2Om}$ and $\delta^{18}O_{OH}$ of the other natural magmatic glasses, which is based on small (≤1.0‰) fractionations between the $\delta^{18}O$ of the silicate and the associated molecular water, and the more moderate $\delta^{18}O$ value of the water that was added (Fig. 6).

### 3.3. $\delta^{18}O$ of water extracted from secondarily hydrated glasses

Table 3 presents analyses of all secondarily hydrated glasses analyzed in this study. Analyses of secondarily hydrated glasses for their $\delta^{18}O$ may provide another simpler end member of our measurements, as the glass is typically hydrated at ambient temperature (Eqs. (1)–(3)) by $H_2O_m$. Isotopic results of this paper confirm this conclusion (Fig. 10).

Fig. 10 illustrates the $\delta^{18}O_{TCEA}$ values relative to the total water concentration of each of these glasses. The total water concentration and δD values were determined in a separate analysis. We can determine the $\delta^{18}O_{Total}$ from Eq. 3 if the relative proportions of $OH^-$ and $H_2O_m$ are known or assumed. For example, we utilize the assumption of little to no secondary water as $OH^-$ being present in the environmentally hydrated Lava Creek Tuff (LCT) glasses.

**Table 4**
Data and sources for temperature, chemistry, speciation, and δD used for $\delta^{18}O$ calculations.

| Sample name | Magmatic temperature | Chemistry data | Relative $H_2O_m$ and $OH^-$ | Bulk silicate $\delta^{18}O$ | δD and total water |
|---|---|---|---|---|---|
| Cleetwood | Druitt and Bacon (1989): 887 °C | Nolan and Bindeman (2013) rhyolite | Newman and Lowenstern (2002) $OH^- = 0.2$ wt% $H_2O_m = 0.01$ wt% | Measured (this study): 6.7‰ | Measured (this study $H_2O_t = 0.21$ wt% $\delta D = -125$‰ |
| IDDP | Zierenberg et al. (2012): 885 °C | Zierenberg et al. (2012) rhyolite | Zierenberg et al. (2012) $OH^- = 1.2$ wt% $H_2O_m = 0.59$ wt% | Zierenberg et al. (2012): 3.1‰ | Measured (this study) and Zierenberg et al. (2012) $H_2O_t = 1.77$ wt% $\delta D = -118$‰ |
| D2 | Bindeman et al. (2013): 900 °C | Seligman et al. (2018) dacite | Ihinger et al. (1999) $OH^- = 1.9$ wt% $H_2O_m = 0.43$ wt% | Bindeman et al. (2013): 4.96‰ | Bindeman et al. (2013) $H_2O_t = 2.33$ wt% $\delta D = -76$‰ |
| VF-74-45 | Rose Jr. et al. (1978): 900 °C | Rose Jr. et al. (1980) andesite | Newman and Lowenstern (2002) $OH^- = 0.42$ wt% $H_2O_m = 0.05$ wt% | Measured (this study): 6.7‰ | Seligman et al. (2016) $H_2O_t = 0.47$ wt% $\delta D = -86$‰ |
| 42-Cordova | Estimated from Nye and Turner (1990): 975 °C | Swanson et al. (1995) andesite | Newman and Lowenstern (2002) $OH^- = 0.51$ wt% $H_2O_m = 0.08$ wt% | Estimated from Nye and Turner (1990): 6.2‰ | Seligman et al. (2016) $H_2O_t = 0.57$ wt% $\delta D = -89$‰ |
| 57-Ashton | Estimated from Nye and Turner (1990): 975 °C | Swanson et al. (1995) andesite | Newman and Lowenstern (2002) $OH^- = 0.51$ wt% $H_2O_m = 0.08$ wt% | Estimated from Nye and Turner (1990): 6.2‰ | Seligman et al. (2016) $H_2O_t = 0.58$ wt% $\delta D = -93$‰ |
| Mt. Mazama | NA | Nolan and Bindeman (2013) rhyolite | Nolan and Bindeman (2013) $OH^- = 0.3$–$1.0$ wt% $H_2O_m = 0.1$–$2.8$ wt% | Measured (this study): 6.2–6.7‰ | Measured (this study) $H_2O_t = 0.4$–$3.8$ wt% $\delta D = -93$‰ |
| Hrafntinnusker | NA | Martin and Sigmarsson (2007) rhyolite | Martin et al. (2017) $OH^- = 0.7$–$1.7$ wt% $H_2O_m = 2.8$–$3.9$ wt% | Martin and Sigmarsson (2007): 3.87‰ | Martin et al. (2017) $H_2O_t = 3.5$–$5.5$ wt% $\delta D = -107$ to $-122$‰ |

To correct for pre-existing magmatic water in the glass (e.g. Seligman et al., 2016), we utilize a $\delta^{18}O$ magmatic water correction by taking into account the small proportion of $OH^-$ that is always present in degassed rhyolitic glass tephra in 0.1–0.3 wt% concentrations. These new values are shown in Fig. 10c, and illustrate that the removal of 0.3 wt% of residual magmatic water causes a small (<1‰) decrease in $\delta^{18}O$ values of our secondarily hydrated glasses, where glasses that have less secondary (molecular) water have the largest shift in $\delta^{18}O$ values following a magmatic correction.

Fig. 10 demonstrates a rather diverse set of $\delta^{18}O$ of extracted water values from secondarily hydrated glasses, but we can confidently observe that: 1) most $\delta^{18}O_{TCEA}$ and $\delta^{18}O_{Total}$ values are generally isotopically negative, and are much lower in $\delta^{18}O$ than their associated bulk silicate; 2) all $\delta^{18}O_{Total}$ values are heavier than the −11.2‰ (Hrafntinnusker) and −12.5‰ (Mt. Mazama) local meteoric waters; 3) generally, the LCT and the Hrafntinnusker glasses (hydrated at elevated temperatures >150 °C; Martin et al., 2017), show an increase in $H_2O_t$ (0.6 wt% and 3.0 wt% respectively) associated with an increase in the $\delta^{18}O$ of the extracted water (6‰ and 4‰ respectively). This result is opposite the outcome shown for δD during secondary hydration (Fig. 2 of Seligman et al., 2016; Martin et al., 2017) where the addition of water leads to either a constant or decreasing δD (36‰ and 15‰ respectively for LCT and Hrafntinnusker glasses), depending on the geographic location of hydration (Fig. 10).

## 4. Discussion

### 4.1. The utility of the TCEA to measure the $\delta^{18}O$ of extracted water

The large dataset for standards presented here (Appendix) demonstrates that the TCEA may be utilized to determine the $\delta^{18}O$ value of water extracted with a per mil precision from a variety of solids. Such precision on single measurements is similar to earlier attempts of thermal decomposition by Hamza and Epstein (1980), Girard and Savin (1996), and Clayton and Mayeda (2009). However, the TCEA permits easy replication and reduction of errors by increasing the number of samples and is much quicker and easier analytically. We also suggest that careful consideration of the complexities that come with analyses of Fe-bearing oxides, especially in samples with water concentration <0.5 wt% is required in the future. Future tests and experimentation could open a wide range of isotopic analyses for hydrous silicates, especially as this method continues to be refined.

We can compare our TCEA results to previous methods that measured $\delta^{18}O$ in water extracted from silicates. In Fig. 11 we compare our $10^3\ln\alpha_{phyllosilicate\text{-}OH}$ values for our biotites (BUD and NBS30), muscovite (RUH2), brucite, and kaolinite to those determined by previous researchers using the increment method (Savin and Lee, 1988; Zheng, 1993a, 1998), Density-Functional Theory (DFT) (Méheut et al., 2007), and partial fluorination (Hamza and Epstein, 1980). Since the $10^3\ln\alpha$ value varies with temperature, and we do not know the closure temperature of our phyllosilicates, we compare our $\delta^{18}O_{OH}$ values to a range of temperatures (200–500 °C) from the literature. Our $\delta^{18}O_{OH}$ values overlap with published values, with the exception of our biotite $\delta^{18}O$ values that fall just outside of the range of published values between 200 and 500 °C, illustrating that our method is comparable to methods previously utilized and tested.

### 4.2. Understanding the $\delta^{18}O$ values of magmatic water extracted from volcanic glasses and trends of volcanic degassing

This study utilizes a new dataset for $10^3\ln\alpha$ and known high temperature fractionations between water and volcanic glass to compute the $\delta^{18}O$ effects on the volcanic degassing trend for oxygen isotopic ratios and combines it with δD analyses for the same samples (Fig. 8). We note a decrease in $\delta^{18}O$ with a decrease in water concentration for basalt, andesite, dacite, and rhyolite glasses. This is similar to hydrogen isotopic trends of degassing (e.g. Newman et al., 1988; Castro et al., 2014) that illustrate a decrease in δD with decreasing wt% water, which is based on the preferential degassing of $^2H$ relative to $^1H$ with a water molecule. The decreasing $\delta^{18}O_{Total}$ with decreasing water may involve a similar process of preferential open system degassing of $^{18}O$ relative to $^{16}O$, similar to the preferential degassing of deuterium. Furthermore, at magmatic temperatures, $10^3\ln\alpha_{silicate\text{-}H2Ot}$ is typically negative (Friedman and O'Neil, 1977). This is illustrated by our data overlapping with the calculated $\delta^{18}O$ degassing trends in Figs. 7 and 8.

As is shown in Fig. 8, felsic glasses have a larger decrease in $\delta^{18}O$ values (5‰ shift), relative to mafic glasses (3‰ shift) during degassing from 4.5 to 0.1 wt% $H_2O_t$, even though the shift in δD values is the same for both compositions. This is likely caused by the difference in normative (e.g. CIPW norm) mineral assemblages between mafic and felsic glasses, and leads to lower $\delta^{18}O$ values of associated waters of felsic glasses, relative to mafic glasses due to the composition induced difference in $10^3\ln\alpha_{silicate\text{-}H2Ot}$ values.

### 4.3. $\delta^{18}O_{Total}$ trends in relation to δD trends of secondary hydration

The secondary hydration trend of the Icelandic Hrafntinnusker glasses, which were hydrated at an estimated 150 °C (Martin et al.,

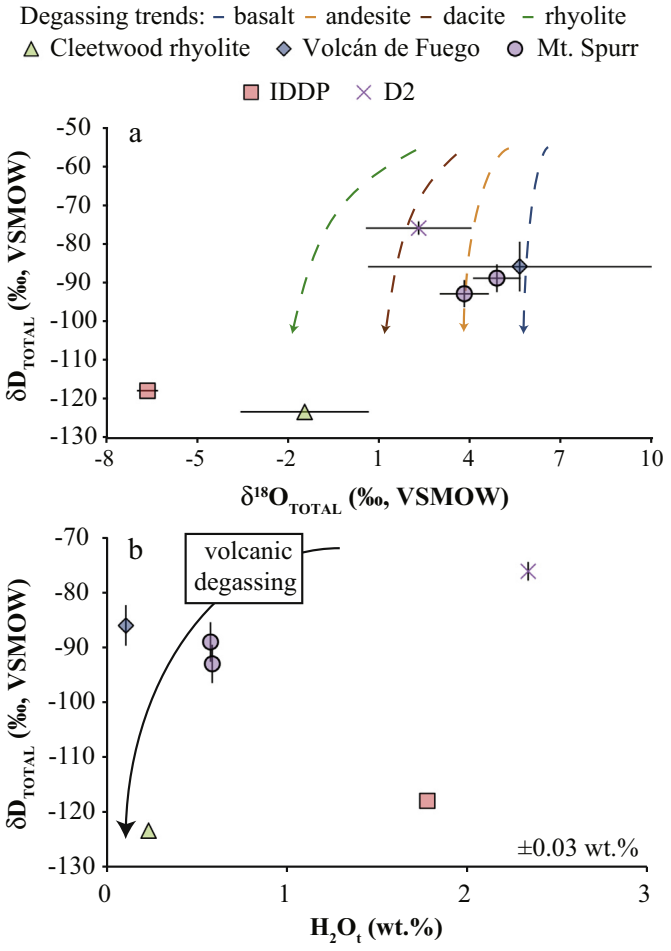


**Fig. 8.** Relationships between water isotopes for water-within-glass and total water concentration. a) δD relative to the $\delta^{18}O_{Total}$, where the $\delta^{18}O$ values have been standard corrected. Notice that both $\delta^{18}O_{WIG}$ and δD decrease with continued degassing. b) $\delta D_{Total}$ relative to the total water concentration, which shows the trends between the hydrogen isotopes and the total water concentration. The volcanic degassing trend here is drawn using data from Newman et al. (1988) and Castro et al. (2014). Note that all our glasses fall within the degassing trend, except D2 and IDDP, which is are both water undersaturated. Error bars are 1 s.d. based on simple error propagation described in the Appendix.

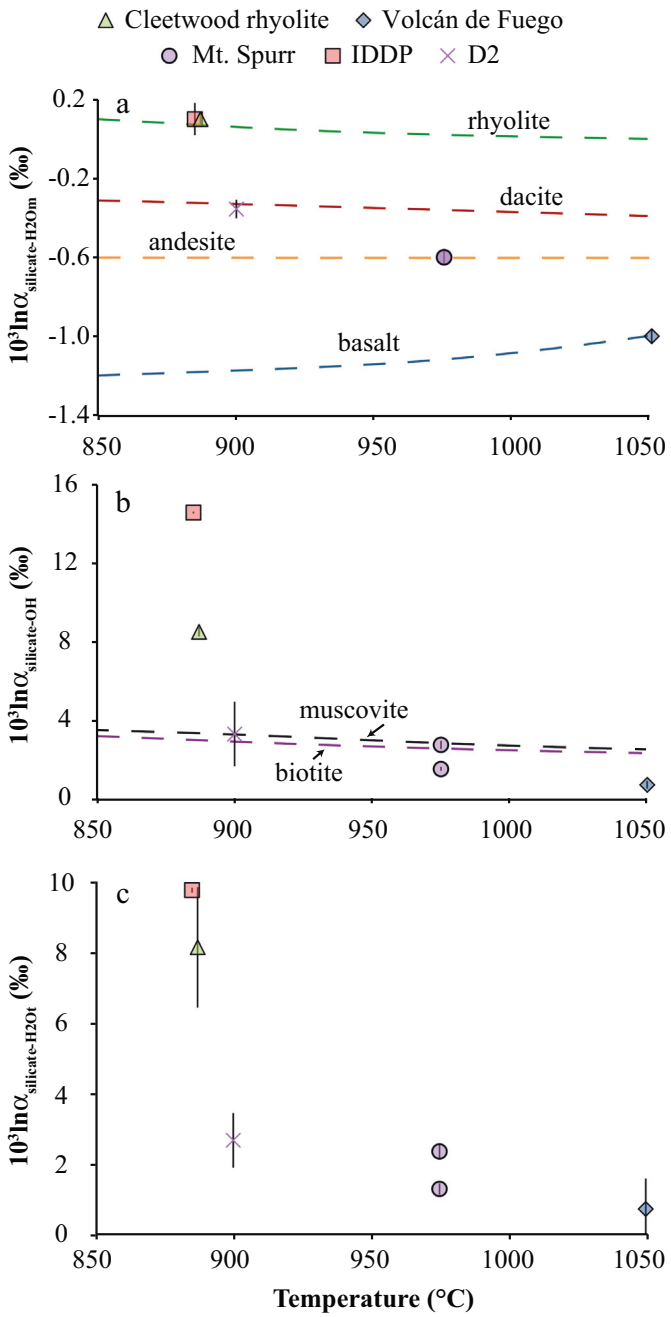


**Fig. 9.** $10^3\ln\alpha$ values of a) $10^3\ln\alpha_{\text{silicate-H2Om}}$, b) $10^3\ln\alpha_{\text{silicate-OH}}$, and c) $10^3\ln\alpha_{\text{silicate-H2Ot}}$ in glass relative to magmatic temperature (measured or taken from literature, see Table 4). All graphs show a decrease in $^{18}O/^{16}O$ fractionation between the silicate and the extracted water with increasing magmatic temperature. In part a), note the $10^3\ln\alpha$ trends for basalt, andesite, dacite, and rhyolite that go directly through our data points, because the $10^3\ln\alpha_{\text{silicate-H2Om}}$ values for our data are from the literature (Zheng, 1991, 1993a; Zhao and Zheng, 2003). In part b), note that the fractionation is larger in our glasses than for muscovite and biotite from Zheng (1993a), which we use as a comparison to our silicate-OH fractionation in our glasses. Error bars are 1 s.d. based on simple error propagation described in the Appendix.

2017), shows an increase in $\delta^{18}O$ with $H_2O_t$, where all the $\delta^{18}O_{Total}$ values remain lower than the $\delta^{18}O_{BG}$ value and higher than the local meteoric water values (Fig. 10). Waters extracted from the glasses hydrated near ambient temperatures (Lava Creek Tuff and Mt. Mazama) are higher in $\delta^{18}O$ than the local precipitation (Fig. 10), but still remain lower in $\delta^{18}O$ than the $\delta^{18}O_{BG}$, except for one Lava Creek Tuff sample that has the highest water concentrations. Likewise, very low (−13 to −10‰) $\delta^{18}O$ values of secondary water were extracted from rapidly hydrated Yellowstone perlites (Bindeman and Lowenstern, 2016), but their $\delta^{18}O$ values were still approximately 4–8‰ heavier than local meteoric waters (−19‰).

We note in Fig. 10 that an increase in water, following secondary hydration, leads to an increase in $\delta^{18}O$ values, trending towards equilibrium. For example, if secondarily hydrated water in glass were in oxygen isotopic equilibrium at low-temperature (20 °C) with −12‰ water, isotopic fractionations would be +33‰, which would drive the host silicate to +21‰. This would likely cause the water in the glass to track an increase in hydration with an upward trend in $\delta^{18}O$. Cerling et al. (1985) demonstrated this with the bulk $\delta^{18}O$ of African ash by showing a dramatic increase in $\delta^{18}O$ with an increase in $H_2O_t$. We see a similar increase in $\delta^{18}O$ with an increase in hydration for our secondarily hydrated samples, but none of the data for water extracted from our hydrated glasses ever reaches the 20 °C equilibrium $\delta^{18}O$ values and remain isotopically light. This may be due to: 1) the glasses not yet being fully hydrated, 2) the secondary hydration process not being solely an equilibrium process (i.e. kinetic fractionation may also play a role during secondary hydration), or 3) the glasses are initially hydrated at higher temperature, which would decrease the isotopic fractionation between the meteoric water and the water in the glass. We already know option 3 is the case for the Hrafntinnusker glasses, which were hydrated at higher temperature, and overlap with their equilibrium values for 150 °C.

## 5. Conclusions

1. This study expands the TCEA CO method to determine the $\delta^{18}O$ of $H_2O_m$, $OH^-$, and $H_2O_t$ of water extracted from volcanic glasses using rapid thermal extraction and conversion to CO at 1450 °C. We consider these analyses to be reliable in determining the $\delta^{18}O$ of waters extracted from volcanic glass containing both primary magmatic and secondary waters, but with per mil precision comparable to previous approaches. However, the TCEA is much quicker and has easier replication, which permits improving precision and good standardization using concurrently run standards.
2. Tests of analyzing water together with glass demonstrate no or limited (<1‰) shifts in the water $\delta^{18}O$ values in glass via reaction with the silicate. The TCEA CO method may be preferred to a two-step process that involves initial extraction of water and then analysis.
3. Our $\delta^{18}O$ of extracted water from phyllosilicates (brucite, biotite, muscovite, and kaolinite) and their computed $10^3\ln\alpha_{\text{pyllosilicate-OH}}$ values of −3 to +6‰ are comparable to theoretical calculations and partial fluorination methods at low temperature, further suggesting minimal analytical effect of water-silicate reaction upon extraction. We note slightly larger $10^3\ln\alpha_{\text{silicate-OH}}$ and $10^3\ln\alpha_{\text{silicate-H2Ot}}$ values for magmatic water in volcanic glasses than for analyzed phyllosilicates, confirming the sense of isotope partitioning of $H_2O_m$ and hydrogen-bound oxygen in silicates. Measured $10^3\ln\alpha_{\text{silicate-OH}}$ values range between +2 and +15‰, while $10^3\ln\alpha_{\text{silicate-H2Om}}$ values range from −1 to 0‰, in agreement with the expected magnitude of fractionations at 850–1050 °C. We also note that the $10^3\ln\alpha_{\text{silicate-H2Ot}}$ of our glasses decreases with increasing estimated magmatic temperature.
4. Using our new $\delta^{18}O$ data, we calculate that the trends for oxygen isotopes of water in magmatic glasses decrease with decreasing water concentration and temperature. This correlates with decreasing $\delta D$ during volcanic degassing, as the departing $H_2O_m$ in fluid phase is heavier in D and $^{18}O$ than the remaining water in the coexisting melt.
5. This study also demonstrates that secondary hydration of volcanic glass, when water is added mostly as $H_2O_m$, initially retains low-$\delta^{18}O$ values of ambient meteoric water. Subsequent residence and hydration causes an increase in $\delta^{18}O_{BG}$ and $\delta^{18}O_{Total}$ values, which is opposite the trend of secondary hydration for hydrogen isotopic ratios. This shows that the trend of oxygen isotopic ratios during

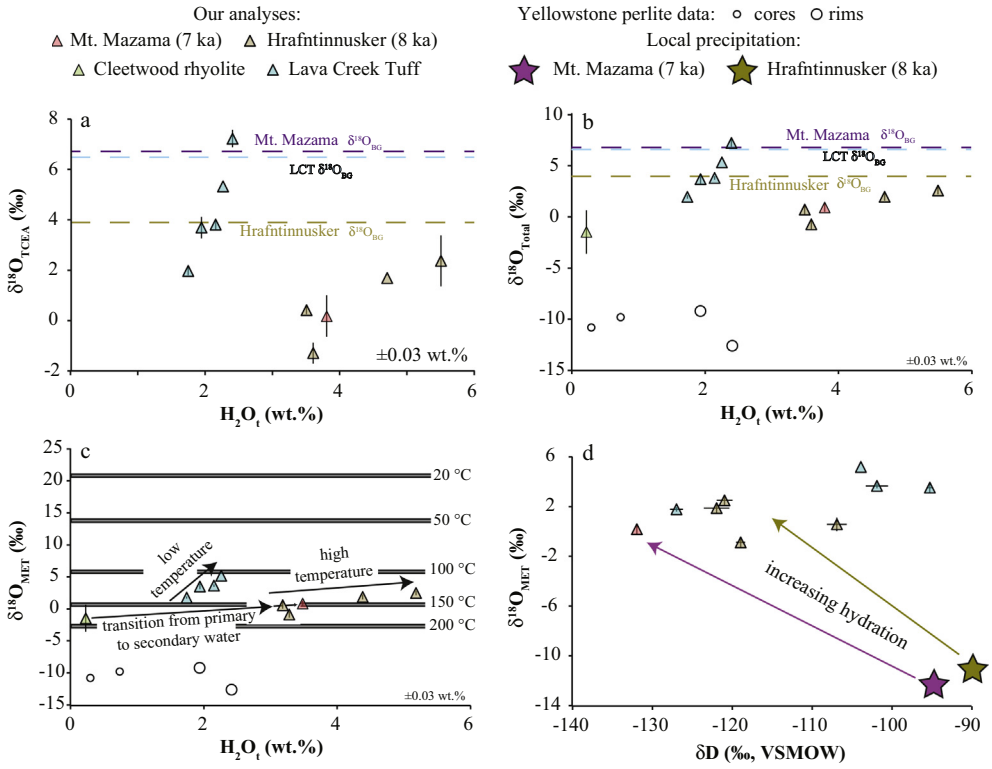


**Fig. 10.** $\delta^{18}O$ of water in glass values extracted from secondarily hydrated glasses relative to the $H_2O_t$ (wt%) of the silicate. a) Values have been standard-normalized to the VSMOW scale. Note that $\delta^{18}O_{WIG}$ values are lower than their respective $\delta^{18}O_{BG}$ (bulk glass) values, reflecting low-$\delta^{18}O_{MET}$ meteoric water hydration. These $\delta^{18}O_{WIC}$ values are also much lower than would be expected for glass-water equilibrium. The LCT samples were collected across the United States, so they have been hydrated with meteoric waters of differing $\delta^{18}O$ values (Table 3), while the Hrafntinnusker glasses in Iceland (hydrated by heated waters) show a trend towards heavier $\delta^{18}O$ and equilibrium values with increasing hydration. Error bars are 1 s.d. based on repeat analyses. b) $\delta^{18}O_{Total}$ values for the Mt. Mazama, Hrafntinnusker, and LCT glasses. c) Computed equilibrium meteoric water values ($\delta^{18}O_{MET}$) showing a greater increase in $\delta^{18}O_{MET}$ for low-temperature hydration than for high-temperature hydration, likely due to the difference in equilibrium $\delta^{18}O$ values, see text for details. d) $\delta^{18}O_{MET}$ versus $\delta D$ for the secondarily hydrated glasses, illustrating the opposing trends between oxygen and hydrogen isotopes during secondary hydration, where $^1H$ is preferred for hydrogen isotopes during secondary hydration, but $\delta^{18}O$ increases with continuing hydration towards heavier $\delta^{18}O$ equilibrium values after initial low-$\delta^{18}O$ water incorporation. The local $\delta^{18}O$ and $\delta D$ of precipitation are from waterisotopes.org. Error bars for b–d are 1 s.d. based on simple error propagation described in the Appendix for.

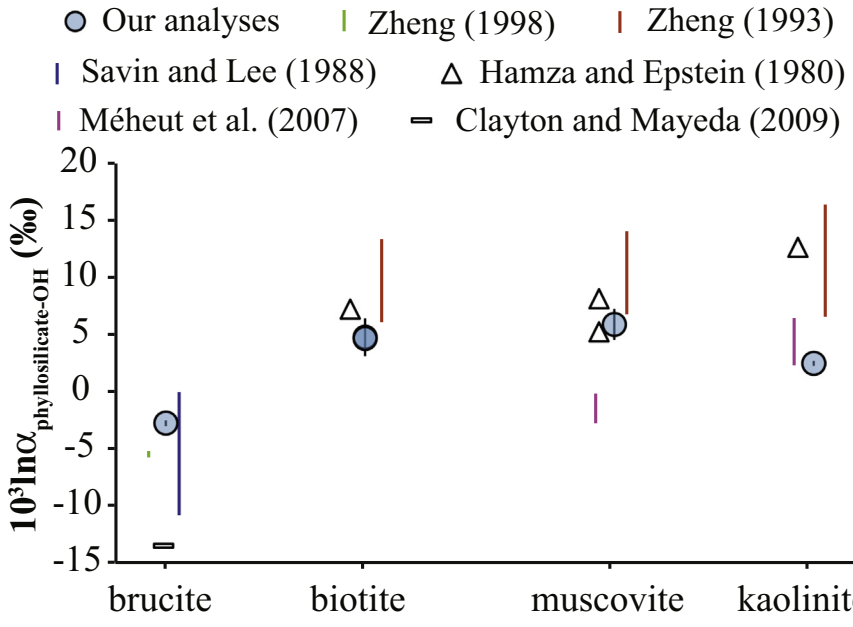


**Fig. 11.** Comparison of our $10^3 ln\alpha_{phyllosilicate\text{-}OH}$ values determined by TCEA in this work for brucite, biotite, muscovite, and kaolinite with measurements by partial fluorination (Hamza and Epstein, 1980; Savin and Lee, 1988), intracrystalline fractionations (Savin and Lee, 1988; Zheng, 1993a, 1998; Méheut et al., 2007), and thermal decomposition (Clayton and Mayeda, 2009). Our $10^3 ln\alpha$ values generally overlap within the temperature ranges shown here. Since we do not know the closure temperature of OH-silicate oxygen exchange in our phyllosilicates, we assume a realistic 200–500 °C temperature range to compare to calculated $10^3 ln\alpha$ values from the literature. When making comparisons, note that fractionation factors from Zheng (1993a) were used to determine our final $10^3 ln\alpha_{phyllosilicate\text{-}OH}$ values. Error bars are 1 s.d. based on simple error propagation described in the Appendix.

secondary hydration may reflect a long-term trend towards water-silicate glass equilibrium with large a $10^3 ln\alpha_{silicate\text{-}H2Ot}$.

## Acknowledgments

We thank Shaul Hurwitz and an anonymous reviewer for constructive reviews. We thank Jim Palandri for lab assistance, Michael Hudak for assistance with sample loading and review, and David Zakharov for assistance with error propagation. We also thank Viorel Atudorei for $\delta^{13}C$ analyses of the glassy carbon from our TCEA, and Erwan Martin for use of his Hrafntinnusker glasses. This work is part of ANS's PhD dissertation, it was supported by the NSF EAR 1822977, a Jack Kleinman Award for volcano research, and a grant from the Geological Society of America.

## Appendix A. Supplementary data

Supplementary data to this article can be found online at https://doi.org/10.1016/j.jvolgeores.2018.12.008.

## References

Anovitz, L.M., Cole, D.R., Riciputi, L.R., 2009. Low-temperature isotopic exchange in obsidian: Implications for diffusive mechanisms. Geochim. Cosmochim. Acta 73 (13), 3795–3806.
Balan, E., Lazzeri, M., Delattre, S., Méheut, M., Refson, K., Winkler, B., 2007. Anharmonicity of inner-OH stretching modes in hydrous phyllosilicates: Assessment from first-principles frozen-phonon calculations. Phys. Chem. Miner. 34, 621–625.
Bao, H., Marchant, D.R., 2006. Quantifying sulfate components and their variations in soils of the McMurdo Dry Valleys, Antarctica. J. Geophys. Res. 111, 1–13.
Bao, H., Koch, P.L., Thiemens, M., 2000. Oxygen isotopic composition of ferric oxides from recent soil, hydrologic, and marine environments. Geochim. Cosmochim. Acta 64, 2221–2231.
Bechtel, A., Hoernes, S., 1990. Oxygen isotope fractionation between oxygen of different sites in illite minerals: a potential single-mineral thermometer. Contrib. Mineral. Petrol. 104, 463–470.
Bindeman, I.N., Lowenstern, J.B., 2016. Low-δD hydration rinds in Yellowstone perlites record rapid syneruptive hydration during glacial and interglacial conditions. Contrib. Mineral. Petrol. 89, 1–24.
Bindeman, I.N., Eiler, J.M., Wing, B.A., Farquhar, J., 2007. Rare sulfur and triple oxygen isotope geochemistry of volcanogenic sulfate aerosols. Geochim. Cosmochim. Acta 71, 2326–2342.
Bindeman, I.N., Kamenetsky, V., Palandri, J., Vennemann, T., 2012. Hydrogen and oxygen isotope behavior during variable degrees of upper mantle melting: example from the basaltic glasses from Macquarie Island. Chem. Geol. 310–311, 126–136.
Brand, W.A., Tegtmeyer, A.R., Hilkert, A., 1994. Compound-specific isotope analysis: extending toward $^{15}N/^{14}N$ and $^{18}O/^{16}O$. Org. Geochem. 21, 585–594.
Cassel, E.J., Breecker, D.O., 2017. Long-term stability of hydrogen isotope ratios in hydrated volcanic glass. Geochim. Cosmochim. Acta 200, 67–86.
Cassel, E.J., Breecker, D.O., Henry, C.D., Larson, T.E., Stockli, D.F., 2014. Profile of a paleo-orogen: high topography across the present-day Basin and Range from 40 to 23 Ma. Geology 42, 1007–1010.
Castro, J.M., Bindeman, I.N., Tuffen, H., Schipper, C.I., 2014. Explosive origin of silicic lava: textural and δD-$H_2O$ evidence for pyroclastic degassing during rhyolite effusion. Earth Planet. Sci. Lett. 405, 52–61.
Cerling, T.E., Brown, F.H., Bowman, J.R., 1985. Low-temperature alteration of volcanic glass: Hydration, Na, K, $^{18}O$, and Ar mobility. Chem. Geol. 52, 281–293.
Clayton, R.N., Mayeda, T.M., 2009. Kinetic isotope effects in oxygen in the laboratory dehydration of magnesian minerals. J. Phys. Chem. A 113, 2212–2217.
Craig, H., 1961. Isotopic variations in meteoric waters. Science 133, 1702–1703.
Crovisier, J., Advocat, T., Dussossoy, J., 2003. Nature and role of natural alteration gels formed on the surface of ancient volcanic glasses (natural analogs of waste containment glasses). J. Nucl. Mater. 321, 91–109.
Dansgaard, W., 1964. Stable isotopes in precipitation. Tellus 16, 436–468.
Dettinger, M.P., Quade, J., 2015. Testing the analytical protocols and calibration of volcanic glass for the reconstruction of hydrogen isotopes in paleoprecipitation. (Memoir of the Geological Society of America; Vol. 212). Memoir of the Geological Society of America (Vol. 212, pp. 261-276). Geol. Soc. Am. https://doi.org/10.1130/2015.1212(14).
Dobson, P.F., Epstein, S., Stolper, E.M., 1989. Hydrogen isotope fractionation between coexisting vapor and silicate glases and melts at low pressure. Geochim. Cosmochim. Acta 53, 2723–2730.
Doremus, R.H., 2000. Water speciation in silicate glasses and melts: Langmuir limited site model. Am. Mineral. 85, 1674–1680.
Druitt, T.H., Bacon, C.R., 1989. Petrology of the zoned calcalkaline magma chamber of Mount Mazama, Crater Lake, Oregon. Contrib. Mineral. Petrol. 101, 245–259.
Eiler, J.M., 2007. "Clumped-isotope" geochemistry – the study of naturally-occurring, multiply-substituted isotopologues. Earth Planet. Sci. Lett. 262, 309–327.
Eiler, J.M., Baumgartner, L.P., Valley, J.W., 1992. Intercrystalline stable isotope diffusion: a fast grain boundary model. Contrib. Mineral. Petrol. 112, 543–557.
Friedman, I., Long, W.D., 1976. Hydration rate of obsidian. Science 191, 347–352.
Friedman, I., O'Neil, J.R., 1977. Data of Geochemistry: Compilation of Stable Isotope Fractionation Factors of Geochemical Interest. 440. US Government Printing Office.
Friedman, I., Gleason, J., Warden, A., 1993. Ancient climate from deuterium content of water in volcanic glass. Geophys. Monogr. 78, 309–319.
Gilg, H.A., Girard, J.P., Sheppard, S.M.F., 2004. Conventional and less conventional techniques for hydrogen and oxygen isotope analysis of clays, associated minerals and pore waters in sediments and soils. Handbook of Stable Isotope Analytical Techniques. 1, pp. 38–61.
Girard, J.P., Savin, S.M., 1996. Intracrystalline fractionation of oxygen isotopes between hydroxyl and non-hydroxyl sites in kaolinite measured by thermal dehydroxylation and partial fluorination. Geochim. Cosmochim. Acta 60, 469–487.
Gong, B., Zheng, Y.F., Chen, R.X., 2008. TC/EA-MS online determination of hydrogen isotope composition and water concentration in eclogitic garnet. Phys. Chem. Miner. 34, 687–698.
Hamza, M.S., Epstein, S., 1980. Oxygen isotopic fractionation between oxygen of different sites in hydroxyl-bearing silicate minerals. Geochim. Cosmochim. Acta 44, 173–182.
Hudak, M.R., Bindeman, I.N., 2018. Conditions of pinnacle formation and glass hydration in cooling ignimbrite sheets from H and O isotope systematics at Crater Lake and the Valley of ten Thousand Smokes. Earth Planet. Sci. Lett. 500, 56–66. https://doi.org/10.1016/j.epsl.2018.07.032.
Ihinger, P.D., Zhang, Y., Stolper, E.M., 1999. The speciation of dissolved water in rhyolitic melt. Geochim. Cosmochim. Acta 63, 3567–3578.
Martin, E., Sigmarsson, O., 2007. Crustal thermal state and origin of silicic magma in Iceland: the case of Torfajökull, Ljósufjöll and Snæfellsjökull volcanoes. Contrib. Mineral. Petrol. 153, 593–605.
Martin, E., Bindeman, I., Balan, E., Palandri, J., Seligman, A., Vollemant, B., 2017. Hydrogen isotope determination by TC/EA technique in application to volcanic glass as a window into secondary hydration. J. Volcanol. Geotherm. Res. 348, 49–61.
McIntosh, I.M., Llewellin, E.W., Humphreys, M.C.S., Nichols, A.R.L., Burgisser, A., Schipper, C.I., Larsen, J.F., 2014. Distribution of dissolved water in magmatic glass records growth and resorption of bubbles. Earth Planet. Sci. Lett. 401, 1–11.
Méheut, M., Lazzeri, M., Balan, E., Mauri, F., 2007. Equilibrium isotopic fractionation in the kaolinite, quartz, water system: prediction from first-principles density-functional theory. Geochim. Cosmochim. Acta 71, 3170–3181.
Méheut, M., Lazzeri, M., Balan, E., Mauri, F., 2010. First-principles calculation of H/D isotopic fractionation between hydrous minerals and water. Geochim. Cosmochim. Acta 74, 3874–3882.
Newman, S., Lowenstern, J.B., 2002. VolatileCalc: a silicate melt-$H_2O$-$CO_2$ solution model written in visual basic for EXCEL. Comput. Geosci. 28, 587–604.
Newman, S., Epstein, S., Stolper, E., 1988. Water, carbon dioxide, and hydrogen isotopes in glasses from the ca. 1340 A.D. eruption of the Mono Craters, California: constraints on degassing phenomena and initial volatile content. J. Volcanol. Geotherm. Res. 35 (1–2), 75–96.
Nolan, G.S., Bindeman, I.N., 2013. Experimental investigation of rates and mechanisms of isotope exchange (O, H) between volcanic ash and isotopically-labeled water. Geochim. Cosmochim. Acta 111, 5–27.
Nye, C.J., Turner, D.L., 1990. Petrology, geochemistry, and age of the Spurr volcanic complex, eastern Aleutian arc. Bull. Volcanol. 52, 205–226.
Pingel, H., Mulch, A., Alonso, R.N., Cottle, J., Hynek, S.A., Poletti, J., Rohrmann, A., Schmitt, A.K., Stockli, D.F., Strecker, M.R., 2016. Surface uplift and convective rainfall along the southern Central Andes (Angastaco Basin, NW Argentina). Earth Planet. Sci. Lett. 440, 33–42.
Poage, M.A., Chamberlain, C.P., 2001. Empirical relationships between elevation and the stable isotope composition of precipitation and surface waters: considerations for studies of paleoelevation change. Am. J. Sci. 301, 1–15.
Rose Jr., W.I., Anderson Jr., A.T., Woodruff, L.G., Bonis, S.B., 1978. The October 1974 basaltic tephra from Fuego Volcano: description and history of the magma body. J. Volcanol. Geotherm. Res. 4, 3–53.
Rose Jr., W.I., Chuan, R.L., Cadle, R.D., Woods, D.C., 1980. Small particles in volcanic eruption clouds. Am. J. Sci. 280, 671–696.
Rowley, D., Pierrehumbert, R., Currie, B., 2001. A new approach to stable isotope-based paleoaltimetry: implications for paleoaltimetry and paleohypsometry of the High Himalaya since the Late Miocene. Earth Planet. Sci. Lett. 188, 253–268.
Rozanski, K., Arguás-Araguás, L., Gonfiantini, R., 1993. Isotopic patterns in modern global precipitation. In: Swart, P.K., Lohmann, K.C., Mckenzie, J., Savin, S. (Eds.), Climate Change in Continental Isotopic Records. Geophysical Monograph 78, pp. 1–36.
Savin, S.M., 1967. Oxygen and Hydrogen Isotope Ratio in Sedimentary Rocks and Minerals. (Ph.D. Thesis). California Institute of Technology.
Savin, S.M., Lee, M.L., 1988. Isotopic studies of phyllosilicates. Rev. Mineral. Geochem. 19, 189–223.
Schütze, H., 1984. Intramolekulare Sauerstoffisotopengeothermemetrie an Hydrosilikaten. Mitt. Zentralinst. Isot 84. Strahlenforsch, Leipzig, pp. 357–363.
Seligman, A.N., Bindeman, I.N., Watkins, J.M., Ross, A.M., 2016. Water in volcanic glass: from volcanic degassing to secondary hydration. Geochim. Cosmochim. Acta 191, 216–238.
Seligman, A.N., Bindeman, I.N., Van Eaton, A., Hoblitt, R., 2018. Isotopic insights into the degassing and secondary hydration of volcanic glass from the 1980 eruptions of Mount St. Helens. Bull. Volcanol. 80 (4), 37. https://doi.org/10.1007/s00445-018-1212-6.
Sharp, Z.D., Atudorei, V., Durakiewicz, T., 2001. A rapid method for determination of hydrogen and oxygen isotope ratios from water and hydrous minerals. Chem. Geol. 178, 197–210.

Sheppard, S.M.F., Gilg, H.A., 1996. Stable isotope geochemistry of clay minerals. Clay Miner. 31, 1–24.
Sveinbjörnsdóttir, A.E., Coleman, M.L., Yardley, B.W.D., 1986. Origin and history of hydrothermal fluids of the Reykjanes and Krafla geothermal fields, Iceland: a stable isotope study. Contrib. Mineral. Petrol. 94, 99–109.
Swanson, S.E., Harbin, M.L., Riehle, J.R., 1995. Use of volcanic glass from ash as a monitoring tool: an example from the 1992 eruptions of Crater Peak, Mount Spurr Volcano, Alaska. U.S. Geol. Surv. Bull. 2139, 129–137.
Taylor, B.E., Westrich, H.R., 1985. Hydrogen isotope exchange and water solubility in experiments using natural rhyolite obsidian. Eos 66, 387.
Vennemann, T.W., Fricke, H.C., Blake, R.E., O'Neil, J.R., Colman, A., 2002. Oxygen isotope analysis of phosphates: a comparison of techniques of analysis of $Ag_3PO_4$. Chem. Geol. 185, 321–336.
Yapp, C.J., 1987. Oxygen and hydrogen isotope variations among geothites (α-FeOOH) and the determination of paleotemperatures. Geochim. Cosmochim. Acta 51, 355–364.
Zhang, Y., 1999. $H_2O$ in rhyolitic glasses and melts: Measurement, speciation, solubility, and diffusion. Rev. Geophys. 37, 493–516.
Zhao, Z.F., Zheng, Y.F., 2003. Calculation of oxygen isotope fractionation in magmatic rocks. Chem. Geol. 193, 59–80.
Zheng, Y., 1991. Calculation of oxygen isotope fractionation in metal oxides. Geochim. Cosmochim. Acta 55, 2299–2307.
Zheng, Y., 1993a. Calculation of oxygen isotope fractionation in hydroxyl-bearing silicates. Earth Planet. Sci. Lett. 120, 247–263.
Zheng, Y., 1993b. Calculation of oxygen isotope fractionation in anhydrous silicate minerals. Geochim. Cosmochim. Acta 57, 1079–1091.
Zheng, Y., 1998. Oxygen isotope fractionation between hydroxide minerals and water. Phys. Chem. Miner. 25, 213–221.
Zierenberg, R.A., Schiffman, P., Barfod, G.H., Lesher, C.E., Marks, N.E., Lowenstern, J.B., Mortensen, A.K., Pope, E.C., Bird, D.K., Reed, M.H., Fridleifsson, G.O., Elders, W.A., 2012. Composition and origin of rhyolite melt intersected by drilling in the Krafla geothermal field, Iceland. Contrib. Mineral. Petrol. 165, 327–347.